



CENTRO DE INVESTIGACIÓN Y DE ESTUDIOS AVANZADOS DEL INSTITUTO
POLITÉCNICO NACIONAL

UNIDAD IRAPUATO

UNIDAD DE GENÓMICA AVANZADA

**Characterization of *low phosphate insensitive 6*: An
Arabidopsis mutant with an impaired Pi starvation
response.**

TESIS QUE PRESENTA

IBT. JONATHAN ODILÓN OJEDA RIVERA

PARA OBTENER EL GRADO DE

MAESTRO EN CIENCIAS

EN LA ESPECIALIDAD DE
BIOTECNOLOGÍA DE PLANTAS

DIRECTORES DE TESIS

DR. LUIS RAFAEL HERRERA ESTRELLA

DR. RUBÉN RELLÁN ÁLVAREZ

IRAPUATO, GUANAJUATO

AGOSTO

2016

INDEX

INDEX	2
AGRADECIMIENTOS	3
ABSTRACT	4
RESUMEN	5
INTRODUCTION	6
Pi deficiency: an agricultural challenge	6
Phosphate Starvation Response in <i>Arabidopsis</i>	9
Precedent: Isolation and genome sequencing of the <i>lpi6</i> mutant of <i>Arabidopsis thaliana</i> ..	15
Objective of the project.....	16
RESULTS	17
Analysis of root development of <i>lpi6</i> seedlings under Pi deficiency conditions	17
Mapping by Sequencing.....	19
Analysis of <i>ALMT1</i> induction under Pi deficiency conditions.....	25
Whole-transcriptome expression profiling of Col-0 and <i>almt1</i> root tips under Pi deficiency conditions.....	26
The <i>almt1</i> mutant phenotype under Pi deficiency conditions can be rescued by external malate addition.....	35
The malate-dependent iron-distribution mechanism that occurs in <i>Arabidopsis thaliana</i> in response to Pi starvation conditions.....	38
DISCUSSION	41
CONCLUSIONS	44
PERSPECTIVES	45
MATERIALS AND METHODS	46
GLOSSARY	52
BIBLIOGRAPHY	53

AGRADECIMIENTOS

Al Colegio Nacional de Ciencia y Tecnología (CONACYT) por la beca No. 396134 (CVU:629657) que se me otorgó para completar este programa de posgrado.

Un agradecimiento al Dr. Luis Rafael Herrera Estrella. No todas las personas tenemos el lujo de decir que trabajamos bajo la supervisión de alguien que ha cambiado el mundo. Por la oportunidad y la experiencia ¡Gracias!

Al Dr. Rubén Rellán Álvarez. Por su paciencia y su guía continua. Por sus múltiples contribuciones al trabajo y por recibirme siempre con una sonrisa ¡Gracias!

Al Dr. Alfredo Cruz Ramírez. Un asesor así no lo tiene ni Obama. Gracias por su guía y por las charlas en su oficina. Por de verdad interesarse por mi formación y mi trabajo ¡Gracias!

A la Dra. Nayelli Marsch Martínez. Gracias por su escucha y sus comentarios sobre el proyecto ¡Gracias!

A la Biol. Araceli Oropeza por aguantarme en el laboratorio, por las charlas a la hora de la comida y por todas las veces, y digo todas, que le pregunté algo y tuvo la disposición para ayudarme ¡Gracias Ara!

A Rossy Gutiérrez por los reactivos, soluciones, puntas y el apoyo en general ¡Gracias Rossy!

Al MC Javier Mora. Miembro del equipo malato y básicamente compañero de proyecto durante estos dos años. Gracias Javi porque fuiste la primera persona que me dio la bienvenida al laboratorio. Parte de este trabajo no hubiera sido posible sin tu ayuda.

A Dr. Javier Raya por la contribución en los experimentos de hierro y en la toma de fotografías. ¡Gracias por tu amabilidad Javi!

A Lenin Yong y Sandra González por su asesoría en cuestiones de transcriptómica y bioinformática. Y al Yong por sus clases de múltiples temas desde Zeldá hasta MySQL.

Al Félix, al Alan, al Chino, a Lolis, a Thelma, al Bello, al Gabriel y a la Rhoscio. Gracias compañeros por las charlas, los pasteles, las gorditas, las apuestas, el zarandeado, los aguachiles, el jaibón... ¡Gracias!

DEDICATORIA

Este trabajo está dedicado a papá y mamá: Odilón Ojeda y María Guadalupe Rivera. Saben que no sería nadie si no fuera por ustedes. Y nada de esto hubiera sido posible. Su apoyo incondicional es un pilar central en mi vida ¡Gracias por recibirme aquella vez que llegue de San Luis Potosí, les acuso a través del presente que me he levantado y estoy caminando con paso firme!

En segundo quiero dedicarlo a mis hermanos Christopher y Miriam y darles las gracias por su apoyo y su aliento.

En tercero quiero dedicarlo a Melisa Aboytes, mi novia, por su apoyo que ha sido enorme. Eres sin duda el otro pilar que me sostiene. Gracias por el aliento, por invitarme a no desesperar. Por estar ahí conmigo a cada paso que di en este trabajo.

ABSTRACT

Phosphorus (P) is an essential element for life, plants assimilate P in its organic form as phosphate (Pi). Being sessile organisms in a changing environment, the phenotypic plasticity of plants in response to nutrient availability is vital for their survival. Systemic transcriptional responses to Pi starvation in plants are controlled by the transcription factor PHR1¹ and have been extensively characterized in the model plant *Arabidopsis thaliana*²⁻⁴. A Root Apical Meristem (RAM) exhaustion program that precedes the inhibition of primary root elongation, an increase in lateral root density and the emergence of root hairs has been reported in the *Arabidopsis thaliana* Col-0 ecotype^{5,6}. Modifications of root architecture under Pi deficiency conditions, also known as the local response to Pi starvation^{2,7}, enhance *A. thaliana* root area of top soil exploration, maximizing nutrient intake when Pi is scarce⁸⁻¹⁰. Absence of such traits in an EMS-induced *low phosphate insensitive 6 (lpi6)* mutant line of *Arabidopsis* encouraged us to study the mechanism underlying a complete absence of the local response to Pi starvation in *lpi6* plants. Mapping by sequencing revealed that the *ALUMINUM ACTIVATED MALATE TRANSPORTER 1 (ALMT1)*, a gene that is critical for aluminum toxicity tolerance in *Arabidopsis*^{11,12}, is mutated in *lpi6*. Root morphology analysis of a T-DNA *ALMT1* knock-out line confirmed the absence of a root architectural response in *almt1* seedlings grown under Pi deficiency conditions. Whole-genome transcriptome analysis revealed the systemic response to be active in the roots of Col-0 and *almt1* seedlings. A transcriptional upregulation of cell-wall related processes, that have been demonstrated to be involved in the inhibition of cell growth and iron accumulation in the root⁹¹⁻⁹⁶, was observed to happen in Col-0 root tips under Pi deficiency conditions. Such response was absent in *almt1* root tips. Our transcriptomic analysis offers new insights into the molecular components of the root architectural response to Pi starvation in *Arabidopsis*. Malate supplementation of the medium revealed the striking reversibility of the mutant phenotype under Pi deficiency conditions. Iron-staining of Col-0 and *almt1* root tips suggests a direct role of malic acid in the iron-dependent regulation of RAM-exhaustion under Pi deficiency conditions that has been reported in *Arabidopsis*¹³. An unprecedented role of *ALMT1* in the Pi starvation response is reported. Our results spur the finding of a key molecular component that triggers the root architectural response to Pi starvation in *Arabidopsis thaliana*.

RESUMEN

El fósforo es un elemento esencial para la vida, las plantas lo asimilan en su forma inorgánica como fosfato. Siendo organismos sésiles, la plasticidad fenotípica de las plantas es una característica clave para su supervivencia. Las respuestas sistémicas a la carencia de fósforo en plantas son orquestadas por el factor de transcripción PHR1¹ y han sido estudiadas extensivamente en la planta modelo *Arabidopsis thaliana*²⁻⁴. En el ecotipo Col-0 de *Arabidopsis*, se ha reportado un programa de agotamiento meristemático que precede la inhibición del crecimiento de la raíz primaria, un incremento en la densidad de raíces laterales y una mayor producción de pelos radiculares^{5,6}. También conocidas como la respuesta local a la carencia de fósforo^{2,7}, las modificaciones del sistema radicular incrementan el área de exploración del suelo de la planta y le permiten a *Arabidopsis* maximizar la absorción de nutrientes cuando el fósforo es escaso⁸⁻¹⁰. La ausencia de la modificación radicular en plantas de la línea *insensible a la carencia de fósforo 6 (lpi6)* crecidas en condiciones de deficiencia de fosfato despertaron nuestro interés por caracterizar el fenotipo mutante de *lpi6*. El mapeo por secuenciación nos permitió identificar a *ALUMINUM ACTIVATED MALATE TRANSPORTER 1 (ALMT1)*, un transportador de malato clave en el mecanismo de tolerancia a la toxicidad por aluminio en *Arabidopsis*^{11,12}, como el gen mutado en *lpi6*. Un análisis de una línea mutante insercional de *ALMT1* reveló una ausencia de respuesta local a la carencia de fósforo. Un análisis de transcriptoma en puntas de raíz reveló que la respuesta sistémica a la carencia de fósforo que es dependiente de PHR1 permanece activa en plántulas de Col-0 y *almt1*. Una inducción de los procesos de regulación de pared celular, que se ha demostrado están involucrados en la inhibición del crecimiento celular y la acumulación de hierro en la raíz⁹¹⁻⁹⁶, se observó en puntas de raíz de plántulas Col-0 lo que no sucedió en plantas mutantes *almt1*. La suplementación de malato al medio reveló la reversibilidad del fenotipo de *almt1* bajo condiciones de carencia de fósforo. La tinción de hierro de raíces de plantas Col-0 y *almt1* sugiere un rol directo del malato en la activación del programa de agotamiento del meristemo que se ha demostrado es dependiente de la distribución de hierro¹³. Nuestros resultados soportan un rol sin precedentes de *ALMT1* como un componente clave para la modificación del sistema radicular en respuesta a la carencia de fósforo en *Arabidopsis thaliana*.

INTRODUCTION

Pi deficiency: an agricultural challenge

Phosphorus (P) is an essential element for life. Living organisms require phosphorus to perform crucial biological processes such as the biosynthesis of nucleic acids and membranes, energy metabolism, cellular signaling, enzymatic regulation and photosynthesis. Plants, as other living organisms, cannot survive without a reliable source of phosphorus.

Agricultural soils must have a sufficient amount of phosphorus that allows plants to develop properly, but most of the agricultural soils have a P deficiency problem. It is calculated that approximately 5.7 billion hectares of land, which equals to 67% of the total farmland available worldwide, have phosphorus deficiency¹⁴. Nitrogen is another essential macronutrient for crop production, nonetheless, its supply is effectively unlimited as its life cycle can be measured in years while the phosphorus cycle is measured in millennia and P reserves are scarce and limited¹⁵⁻¹⁷. The world's main source of P for fertilizer production is phosphate rock whose demand has increased dramatically in the last century as illustrated in Fig. 1:

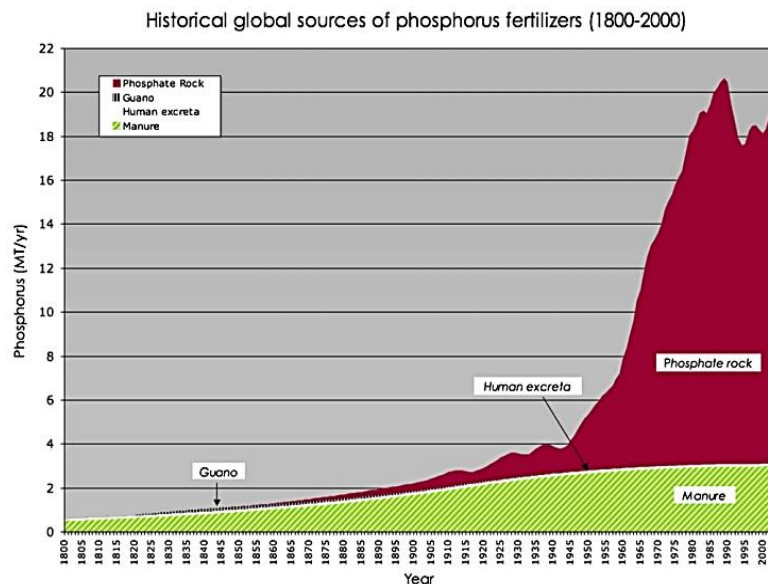


Figure 1 (last page). **Phosphate rock demand has increased exponentially over the last two centuries**¹⁶. The demand of the respective phosphorus sources is depicted in colors. Graph illustrates an approximate the Millions of Tons of Demanded phosphorus (MT/yr) per year worldwide vs the year.

So, on one hand we have an exponentially increasing demand of phosphorus and on the other hand we have a limited and scarce source of P which is predicted to be depleted by 2120 as illustrated in Fig. 2:

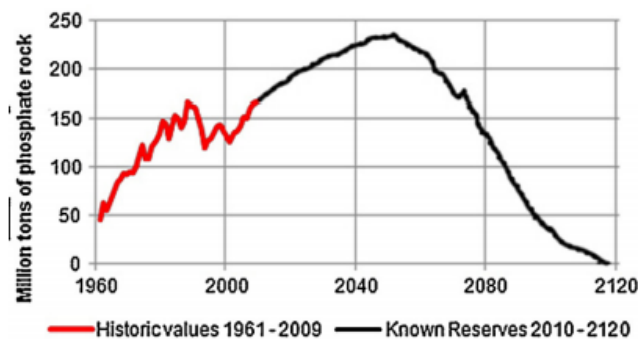


Figure 2. Phosphate rock reserves are predicted to be depleted by the year 2120¹⁸. The millions of tons of known phosphate rock reserves are illustrated to the year 2009 in red color. A forecast of the phosphate rock reserves behavior is presented in black color.

Thus, phosphorus scarcity arises as an imminent challenge, but supplying phosphorus to plants is not the only problem in agricultural practices as phosphorus can be in an optimal concentration in the soil and still remain unavailable for plant absorption. Since plants assimilate phosphorus only in its inorganic form¹⁰ as phosphate (Pi ; H_2PO_4^- or HPO_4^-), and Pi is one of the least available macronutrients in the soil, Pi unavailability comes up as an additional complication of the Pi supply chain in agricultural practices. Pi unavailability is the result of the poor mobility of this element in the soil¹⁹. Pi is quickly fixed in the soil as it reacts with a variety of mineral ions to form low solubility compounds in a pH dependent fashion^{20,21}. Pi reacts with aluminum and iron in acid soils or magnesium and calcium in alkaloid soils to form compounds that fixate phosphorus in soil making it unavailable for plant absorption²¹. The application of excessive amounts of P-based fertilizer that exceed the soil capacity of Pi fixation renders the supply of phosphorus fertilizer as an inefficient process that endangers ecosystems through leaching of the Pi excess⁸⁵.

The application of nitrogen fertilizers has been demonstrated to enhance the water solubility of the fixated inorganic phosphorous compounds causing Pi leaching and the eutrophication of rivers and lakes^{85,86}. Of the massive amounts of fertilizers that are applied on a regular basis to crops only 20 to 30% is assimilated by the plants²², the rest is leached to the lakes, rivers and oceans causing ecological damage. Pi use efficiency through genetic improvement of field crops rises as key tool to improve Pi uptake by plants and prevent environmental damages caused by Pi leaching as illustrated in Fig. 3.

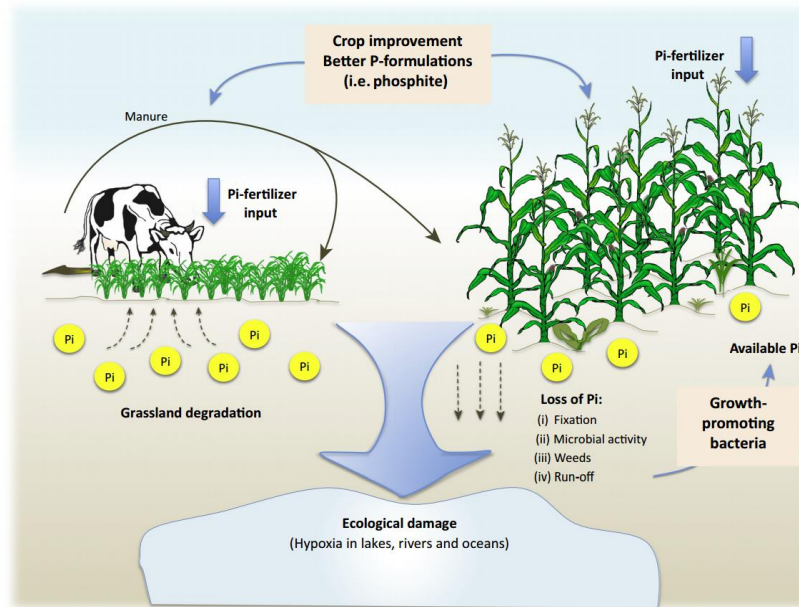


Figure 3. Pi-use efficiency could reduce Pi-leaching losses²². Genetic engineering of field crops along with a better formulation of Pi-based fertilizers could improve Pi-use efficiency in agricultural practices and prevent further ecological damages.

Plant improvement strategies including classical breeding and genetic engineering as a possible solution to the Pi challenge. The studies of the genetic networks of regulation behind Pi starvation in plants take a vital importance as they are essential for the selection of gene candidates for gene edition or transgenic technologies oriented to produce enhanced plants with a higher tolerance to Pi starvation.

Phosphate Starvation Response in *Arabidopsis*

***Arabidopsis* as a model of study**

Being low Pi availability a common problem in soils worldwide, plants have evolved several adaptive responses to cope with Pi shortage. Adaptive responses are known as the Pi starvation response, and comprehend a myriad of biochemical, morphological and physiological changes oriented towards Pi use efficiency, recycling and acquisition.

The main adaptive responses to low Pi availability include the alteration of root architecture and the activation of long distance signaling pathways, such strategies are oriented to improve the capacity of the plant to acquire Pi and to use it in a more efficient manner in order to maintain internal Pi homeostasis¹⁹. Plant responses to Pi starvation have been extensively characterized in the model plant *Arabidopsis thaliana*, specifically in the accession Columbia-0 (Col-0), which displays a contrasting phenotype in function of Pi availability⁶ as illustrated in Figure 4:

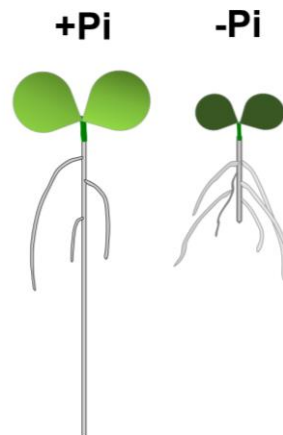


Figure 4. **Scheme of *Arabidopsis* accession Col-0 seedlings under grown under Pi sufficiency (+Pi) and Pi deficiency (-Pi) conditions.** Observable traits of seedlings grown under Pi deficiency conditions include an increased production of anthocyanin's in shoots denoted by a brown-red color, a shorter primary root and a major number of lateral and hair roots than the seedlings grown under +Pi conditions.

Local and systemic responses to Pi starvation in *Arabidopsis*

A dissection of local and systemic responses to Pi starvation has been described in *Arabidopsis*^{2,7}. Alterations of root architecture, also known as the local response of the plant to Pi starvation, include the inhibition of primary root growth, a switch of the RAM to a determinate exhaustion program, an increase in lateral root density and an enhancement in the production of root hairs^{6,23}. On the other hand, long distance signaling responses, or systemic responses, are dependent of the internal Pi concentration in the plant and include the activation of genes whose products catalyze the recycling of internal Pi, Pi transport and Pi metabolism optimization²⁴.

A scheme that summarizes *Arabidopsis* response to Pi starvation is presented in Figure 5.

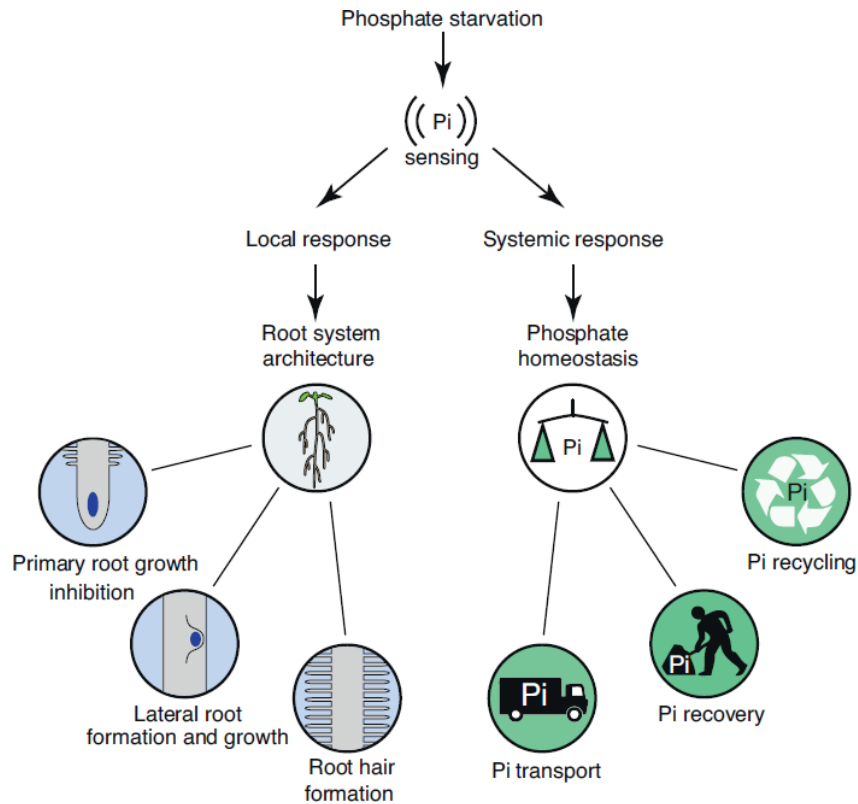


Figure 5. Pi starvation response in *Arabidopsis thaliana*⁷. An illustration that resumes the dissection of the local and systemic responses^{2,7}.

Molecular components of the Systemic Response to Phosphate Starvation

In 2001, Rubio et al. published the characterization of an *Arabidopsis* EMS-mutagenized mutant that was unresponsive to Pi deficiency conditions and named it *phosphate starvation response 1 (phr1)*. Characterization of *phr1* revealed it to be a mutant in a gene that codes for a MYB transcription factor which binds to the promoters of several genes induced by Pi starvation¹. The discovery of *PHR1* is one of the keystones in the study of the genetic response to phosphate starvation in vascular plants and it remains as one of the most prominent components of the Phosphate Starvation Response (PSR) in the plant kingdom. *PHR1* is not regulated transcriptionally by Pi starvation¹, but *PHR1* is post-translationally regulated as it is a target of sumoylation by *SIZ1* in response to Pi status²⁵. *PHR1* and *PHR*-like 1 (*PHL1*) transcription factors were reported to control most of *Arabidopsis* transcriptional upregulation of PSR genes. *PHR1* activates the expression of genes that harbor one or more *PHR1*-binding (*P1BS*) motif in their regulatory region. PSR genes with *P1BS* enriched promoters comprehend most of *Arabidopsis* systemic response to Pi starvation².

PHO2, a gene that codes for a ubiquitin E2 conjugase gene, is another key player of the systemic response to Pi starvation in *Arabidopsis*. The Pi-overaccumulator *pho2* mutant was isolated and characterized by Delhaize and Randall in 1995. *PHO2* transcript was shown to be negatively regulated under -Pi conditions by the *PHR1*-induced microRNA *mir399* in a phosphate signaling pathway that regulates a set of PSR inducible genes²⁶. At the N-terminus of several proteins, the SPX-domain (*SIG1-Pho81-XPR1*) is found in all major eukaryotes and are involved in signal transduction²⁷. In plants, SPX-domain containing proteins have been demonstrated to be essential in the maintenance of phosphate homeostasis²⁸. The *Arabidopsis* genome encodes for 20 SPX-domain containing proteins of which 4 genes *SPX1-4* (*At5g20150*, *At2g26660*, *At2g45130* and *At5g15330*) code solely for an SPX-domain. *SPX1* was demonstrated to bind and inhibit *PHR1* in a Pi-dependent manner, as a result it was concluded that the *SPX1/PHR1* module links Pi sensing and signaling²⁹. An example of an SPX-domain bearer protein is found in *PHO1*, an essential protein for root-to-shoot Pi loading^{87,88}, which also plays a key role in the systemic regulation of Pi homeostasis⁸⁹.

PHR1 promotes Pi uptake through the induction of PHT1-like family of high affinity phosphate transporters³⁰. It also promotes Pi scavenging through the transcriptional activation of purple acid phosphatases (PAPs) that hydrolyze Pi from a wide variety of Pi-monoesters³¹. Phospholipid substitution, a replacement of membrane phospholipids for sulfo- or galacto-lipids is another plant countermeasure to cope with Pi starvation³², and it has been shown to be under PHR1 transcriptional control^{33,34}. A table with PSR genes that are known to be systemically upregulated by low-Pi availability is presented in Table 1:





	Process	ID	GENE	P1BS	<i>phr1</i>	Function	
	Pi scavenging	AT1G52940	PAP 5			Purple Acid Phosphatase	
		AT2G18130	PAP 11			Purple Acid Phosphatase	
		AT2G27190	PAP 12			Purple Acid Phosphatase	
		AT2G46880	PAP 14			Purple Acid Phosphatase	
		AT3G10150	PAP 16			Purple Acid Phosphatase	
		AT3G17790	PAP 17			Purple Acid Phosphatase	
		AT3G46120	PAP 19			Purple Acid Phosphatase	
		AT3G52820	PAP 22			Purple Acid Phosphatase	
		AT4G13700	PAP 23			Purple Acid Phosphatase	
		AT4G36350	PAP 25			Purple Acid Phosphatase	
		AT1G73010	PS 2			Phosphatase	
		AT1G17710	PECP1			Phosphoethanolamine/phosphocoline phosphatase	
		AT2G02990	RNS 1			RNAse	
	Phospholipid substitution	AT3G03530	NPC 4			Phospholipase C	
		AT3G03540	NPC 5			Phospholipase C	
		AT3G05630	PLD Z			Phospholipase D	
		AT5G20410	MGDG 2			monogalactosyldiacylglycerol synthase	
		AT2G11810	MGDG 3			monogalactosyldiacylglycerol synthase	
		At4g33030	SQD 1			sulfoquinovosyldiacylglycerol synthase	
		AT5G01220	SQD 2			sulfoquinovosyldiacylglycerol synthase	
		AT3G02040	GDPD 1			glycerophosphodiester phosphodiesterase	
		AT5G08030	GDPD 6			glycerophosphodiester phosphodiesterase	
			Transport	AT5G43350	PHT 1;1		
AT5G43370	PHT 1;2					Phosphate transporter	
AT5G43360	PHT 1;3					Phosphate transporter	
AT2G38940	PHT 1;4					Phosphate transporter	
At2g32830	PHT 1;5					Phosphate transporter	
AT5G43340	PHT 1;6					Phosphate transporter	
AT3G54700	PHT 1;7					Phosphate transporter	
AT1G20860	PHT 1;8					Phosphate transporter	
AT1G76430	PHT 1;9					Phosphate transporter	
AT1G73220	AtOCT 1					Organic cation/Carnitine transporter	
AT5G09470	DIC 3					Mitochondrial dicarboxylate carrier	
AT3G23430	PHO 1;H1					Pi translocation	
	Sensing and Signalling			AT3G09922	AtP S1		
		AT5G03545	At 4				
		AT1G29265	mir399a				mic roRNA
		AT1G63005	mir399b				mic roRNA
		AT5G62162	mir399c				mic roRNA
		AT2G34202	mir399d				mic roRNA
		AT2G34204	mir399e				mic roRNA
		AT5G20150	SPX 1				SPX-domain containing protein
		At2g26660	SPX 2				SPX-domain containing protein
		AT2G45130	SPX 3				SPX-domain containing protein
		AT1G08650	AtPPCK 1				Kinase
		AT3G04530	AtPPCK 2				Kinase

Table 1 (last page). Systemic PSR genes. Genes with their respective process, ID and function are listed. Green colored genes in the P1BS column have been reported to have a P1BS¹⁻³. Red colored genes in the *phr1* column have been reported to be downregulated/non-responsive under Pi starvation conditions in the *phr1* mutant line⁴.

Known pieces of the local response to phosphate starvation puzzle

As mentioned earlier, the local response to phosphate starvation comprehends the alterations of root architecture. An inhibition of primary root growth accompanied by an increase of lateral root density and root hair number enhances the root area of soil exploration which maximizes the plant nutrient intake when Pi is scarce¹⁹. A switch of the RAM to a determinate developmental program which is the result of the full differentiation of all the cells in the root stem cell niche, including the initials or stem cells and the Quiescent Center (QC), leads to the inhibition of primary root growth in response to Pi deficiency conditions has been reported in the Col-0 ecotype of *Arabidopsis thaliana*²³, such phenomenon is illustrated in Figure 6:

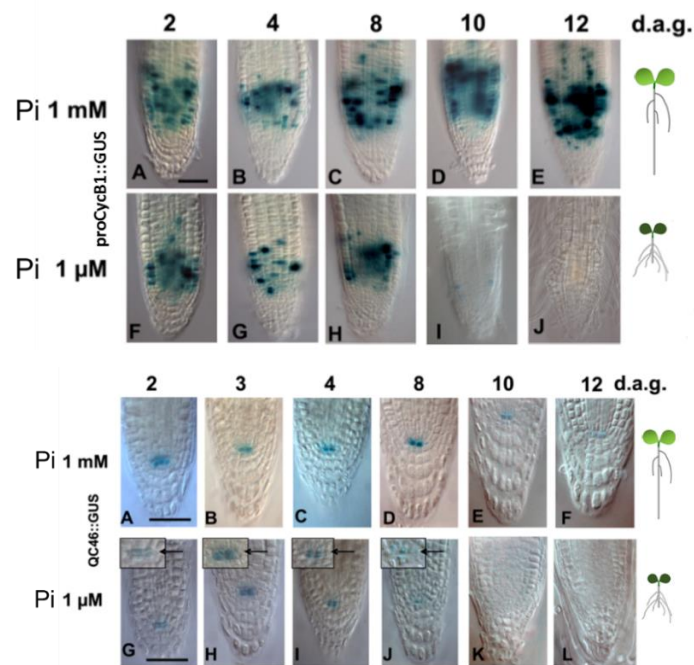


Figure 6. RAM exhaustion program in response Pi deficiency⁵. (A) 12 dag kinetics of the RAM cell cycle arrest depicted by GUS staining of the proCycB1::GUS reporter line. (B) 12 dag kinetics

of the RAM QC differentiation depicted by GUS staining of the QC46::GUS reporter line. Modified from Sánchez-Calderón (2005).

Root tip contact with low phosphate medium has been demonstrated to be essential to elicit the root architectural response to Pi starvation³⁵. A multicopper-oxidase *LPR1*, whose mutant has a long root under Pi-deficiency conditions and a P5-type ATPase *PDR2*, whose mutant is hypersensitive to Pi starvation conditions, have been shown to orchestrate RAM exhaustion in response to Pi-deficiency conditions in *Arabidopsis thaliana*³⁶. Iron has been demonstrated to be critical for primary root inhibition under Pi deficiency conditions³⁷. Furthermore, an iron-dependent callose deposition which inhibits the symplastic transport of transcription factors, such as *SHORTROOT* and *SCARECROW*, has been reported to be essential for RAM exhaustion¹³. A summary of this report is shown in Figure 7:

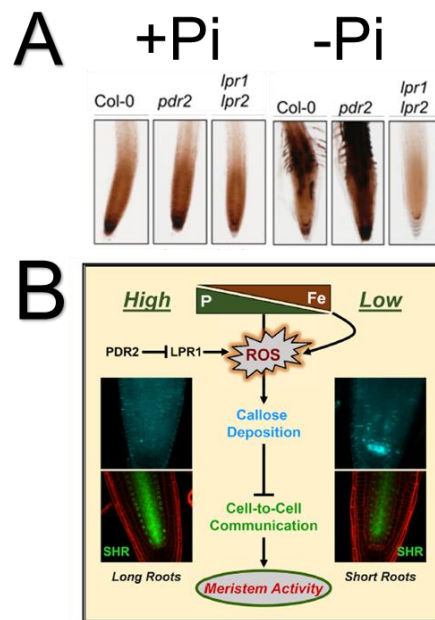


Figure 7. **An iron-distribution dependent mechanism controls RAM exhaustion in response to Pi deficiency conditions in *Arabidopsis*.** (A) Iron distribution changes in the root tip of *Arabidopsis* under Pi deficiency conditions as revealed by 3,3'-Diaminobenzidine (DAB) iron staining of Col-0 and Pi-deficiency-response mutant lines of *Arabidopsis*.

Studies of the local response mutants *lpr1* and *pdr2* have shed some light on the components of the local response recently but ironically have also revealed the complexity behind the RAM developmental program of *Arabidopsis thaliana* under Pi deficiency

conditions. Key players of the local response to Pi starvation remain concealed. In this work, we present the genetic and transcriptomic characterization of a mutant with a long root phenotype under Pi deficiency conditions and report a previously undescribed role of ALMT1 in the local response to Pi starvation in *Arabidopsis thaliana*.

Precedent: Isolation and genome sequencing of the *lpi6* mutant of *Arabidopsis thaliana*.

A screening of ethyl methane sulfonate (EMS)-induced mutants of *Arabidopsis thaliana* with an aberrant response to Pi deficiency (-Pi) conditions was carried out previously in our laboratory (Figure 8A, Mora, J. *unpublished*). One of the isolated lines was named *low phosphate insensitive 6 (lpi6)* as it continued primary root growth under Pi deficiency conditions (Figure 8B). The recessive nature of the mutant was determined by the segregation ratio (3:1) of the F2 offspring of the WT x *lpi6* cross (Figure 8C). Genomic sequencing data from Col-0-like individuals and *lpi6* individuals from the F2 offspring of the Col-0 x *lpi6* cross was obtained (Mora, J. *unpublished*) but remained unmapped.

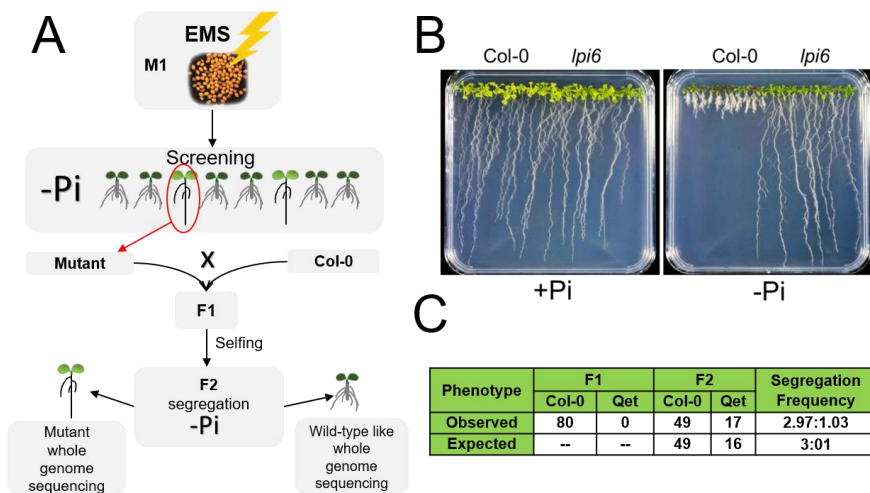


Figure 8. **Isolation of the *low phosphate insensitive 6 (lpi6)* mutant line of *Arabidopsis thaliana*.** (A) Screening of low phosphate response EMS-induced mutants of *Arabidopsis thaliana*. (B) Phenotype of *lpi6* seedlings at 10 days-after-germination (dag). (C) Segregation frequency of the Col-0 X *lpi6* cross under Pi deficiency conditions. *lpi6* phenotype was determined to be caused by a recessive mutation due to a 3:1 wild-type to mutant phenotype segregation ratio.

Objective of the project

To carry out the physiological, cellular and molecular characterization of the *Arabidopsis low phosphate insensitive 6* mutant.

Specific Objectives

1. Identification of the gene responsible for the *low phosphate insensitive 6* phenotype.
2. Physiological characterization of *low phosphate insensitive 6*.
3. Global expression profiling of the *lpi6* mutant to determine the subset of Pi-responsive genes affected in this mutant

Overall experimental strategy of the project:

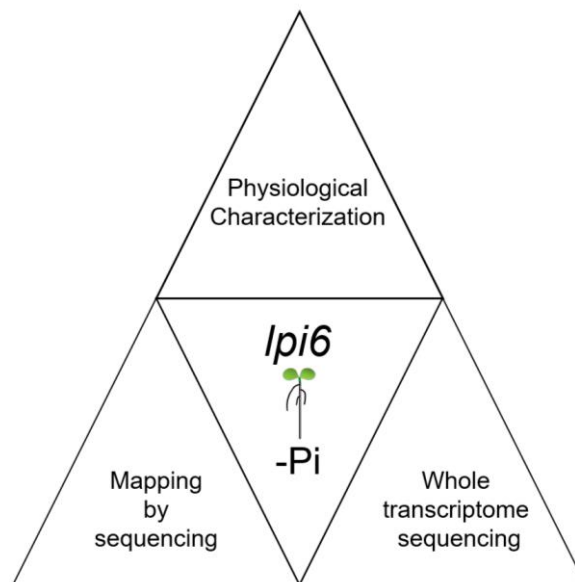


Figure 9. **The overall experimental approach to characterize *lpi6*.** Diagram illustrates the three principal experimental strategies of this project.

RESULTS

Analysis of root development of *lpi6* seedlings under Pi deficiency conditions

Having a mutant with an altered root architectural response to Pi starvation, we began its characterization with a comparative analysis of Col-0 and *lpi6* root traits of seedlings grown under +Pi and -Pi conditions 10 days after germination (dag) (Figure 10).

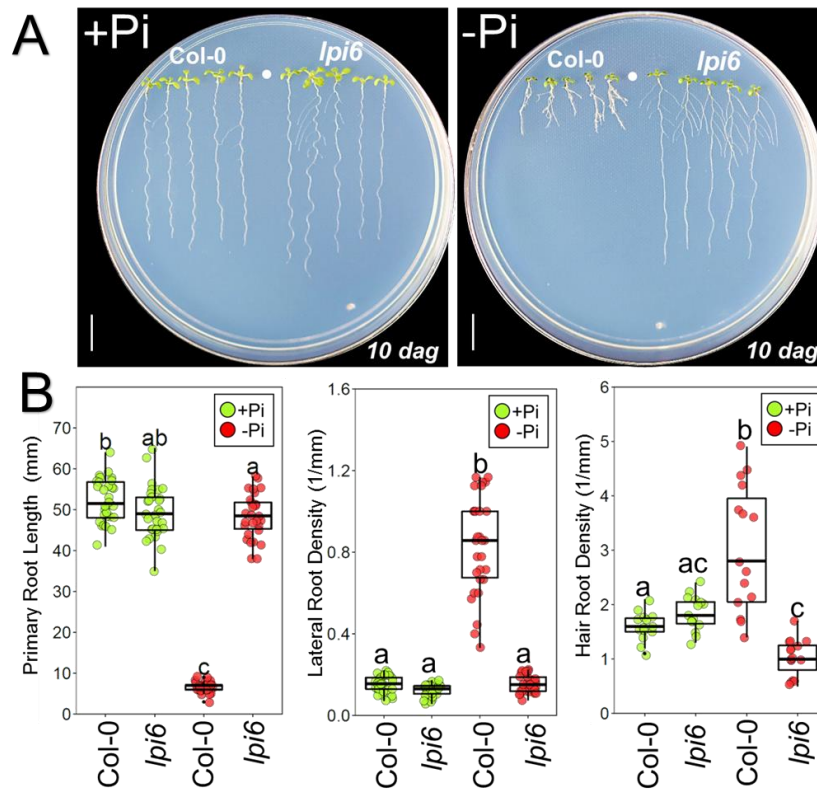


Figure 10. **Root development of Col-0, *lpi5* and *lpi6* seedlings grown under Pi sufficiency and Pi deficiency conditions.** (A) Phenotypes of 10 days-after-germination (dag) Col-0 and *lpi6* seedlings grown under Pi sufficiency (+Pi) and Pi-deficiency (-Pi) conditions. Scale bar equals 1 cm. (B-D) Primary Root Length (B) Lateral Root Density (C) and Hair Root Density (D) of 10 dag Col-0 and *lpi6* seedlings grown under +Pi and -Pi conditions. Lateral and root hair densities are expressed by units by mm of primary root length. Green red dots depict Col-0 and *lpi6* individuals (n=30 from 3

independent experiments), respectively. Statistical groups were determined using a Tukey HSD test (P-value < .05) and are indicated by letters.

A complete shutdown of the local response to Pi starvation in *lpi6* seedlings was evidenced by the sustained primary root growth (Figure 10A, B), the reduced number of lateral roots (Figure 10C) and a lack of root hairs production (Figure 10 D) under Pi deficiency conditions.

The observed *lpi6* root traits pointed to an absence of the RAM exhaustion program that takes place in response to Pi deficiency conditions in *Arabidopsis*²³. Therefore, we studied the expression of the cell cycle activity marker (proCycB1::GUS³⁸) and the quiescent center identity marker (proQC46::GUS³⁸) in the roots of Col-0 and *lpi6* seedlings (Figure 11). At 10 dag, GUS staining of seedlings grown under -Pi conditions revealed proCycB1::GUS (Figure 11A) and proQC46::GUS (Figure 11B) markers to be still active in the primary root of *lpi6* while expression of both markers was not observed in the wild type Col-0 plants.

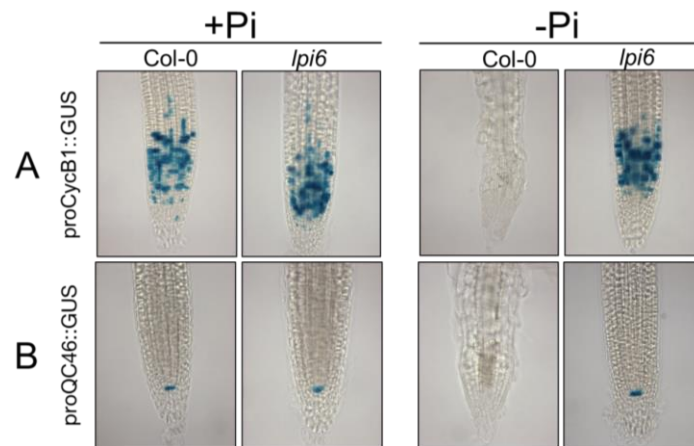


Figure 11. **RAM exhaustion program is not active in the roots of *lpi6* seedlings in response to Pi deficiency conditions.** GUS staining of proCycB1::GUS and proQC46::GUS expression activity in the root apical meristem (RAM) of Col-0 and *lpi6* 10 dag seedlings. Scale bar equals 100 μ m.

Since *lpi6* plants can continue primary root growth under Pi deficiency conditions, they must carry a mutation in a locus which genetic product is essential for the execution of the RAM exhaustion program and the further inhibition of primary root growth.

Mapping by Sequencing

To identify the gene responsible for the *lpi6* mutant phenotype under Pi deficiency conditions, a mapping by sequencing approach (Abe et al. 2012) was used (Figure 12). Such methodology allows to filter mutations that are not responsible for the phenotype, such as EMS-induced heterozygous mutations and it also dismisses variants between the Col-0 material used for mutagenesis and the *Arabidopsis* reference genome available in TAIR (www.arabidopsis.org) (Figure 12).

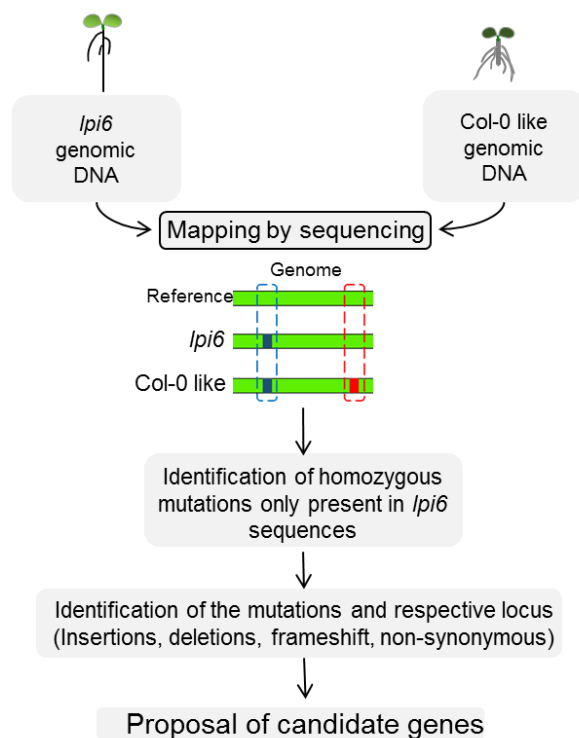


Figure 12. **Mapping by sequencing of the Pi starvation response mutant *lpi6***. Mainly based on Abe et al. 2012³⁹ and Mora, J. (unpublished) methodologies, the strategy for the mapping by sequencing approach is resumed. A quick identification of critical genes in the local response to Pi starvation is allowed using this methodology. Heterozygous mutations, which are not responsible for the phenotype, and variants between the Col-0 material and the *Arabidopsis thaliana* Col-0 reference genome available in TAIR are filtered. Genes with critical roles that could be responsible for the phenotype are selected as candidates.

Results from the mapping by sequencing bioinformatics pipeline (see Materials and Methods), revealed that 11 genes to have a homozygous mutation across the *lpi6* genome (Figure 13A). Having identified the recessive nature of all the mutated loci present in the *lpi6* genome, we proceeded to elaborate a list of candidate genes with information about the gene and the mutation (Figure 13B).

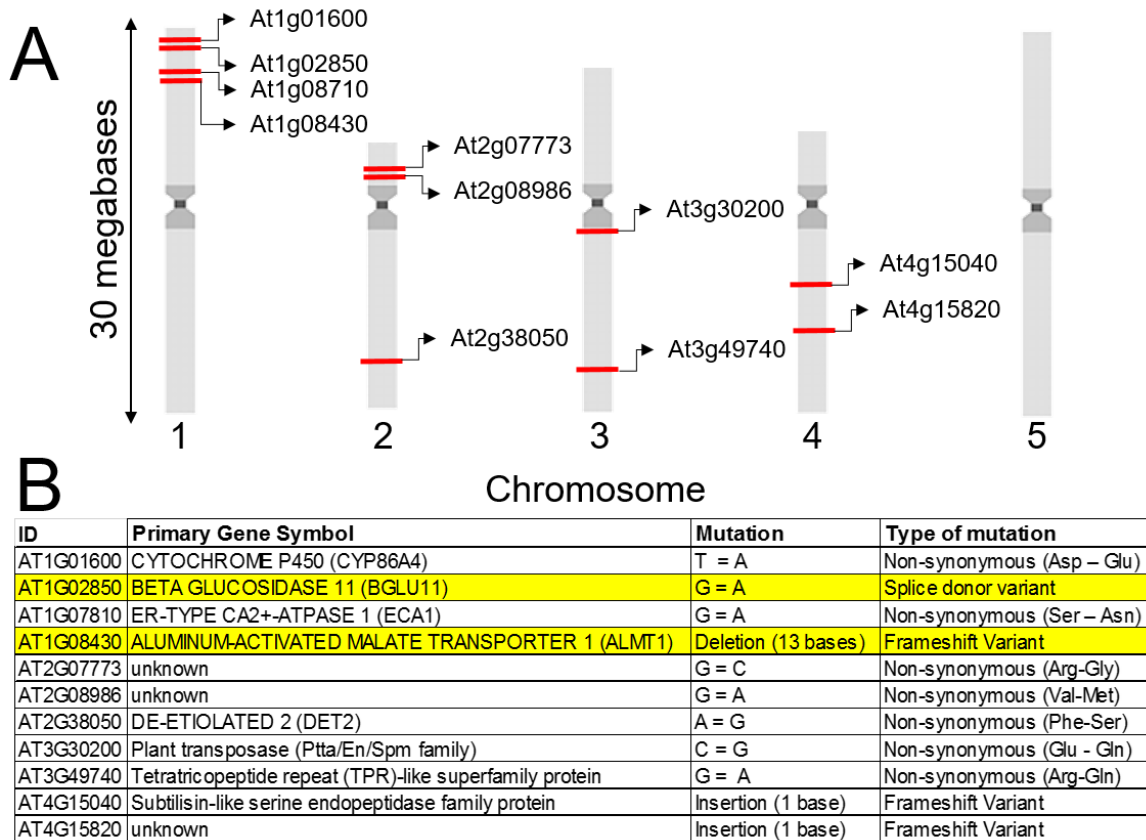


Figure 13. **Homozygous mutations present across several loci the *lpi6* genome as revealed by the mapping by sequencing protocol.** (A) Graphic illustration of the 5 *Arabidopsis thaliana* chromosomes. Mutated loci are depicted by a red bar and their respective ID is indicated. (B) List of mutated genes in the *lpi6* genome. Locus ID, primary gene symbol, mutation and type of mutations are listed.

As aluminum toxicity and phosphate starvation are common stresses in acid soils⁴⁰ we selected At1g08430 (Figure 13B) which is the *ALUMINUM ACTIVATED MALATE TRANSPORTER (ALMT1)* as a gene candidate. The *Arabidopsis ALMT1* has been reported to be induced under aluminum stress conditions¹¹ and its orthologue in soybean has been

implicated in the regulating malate exudation in response to phosphate and aluminum stress conditions⁴¹. The other candidate we selected is At1g02850 which codes for a Beta-Glucosidase 11 of that acts on O-glycosyl compounds⁴² and has been reported to be induced by Pi deficiency conditions⁴³. We requested DNA insertional mutants in At1g08430 (SALK_009629; Col-0 background; *almt1*) and At1g02850 (NASC N25931; Ler background; *glh11*) and performed crosses against *lpi6* to test for genetic complementation (Figure 14).

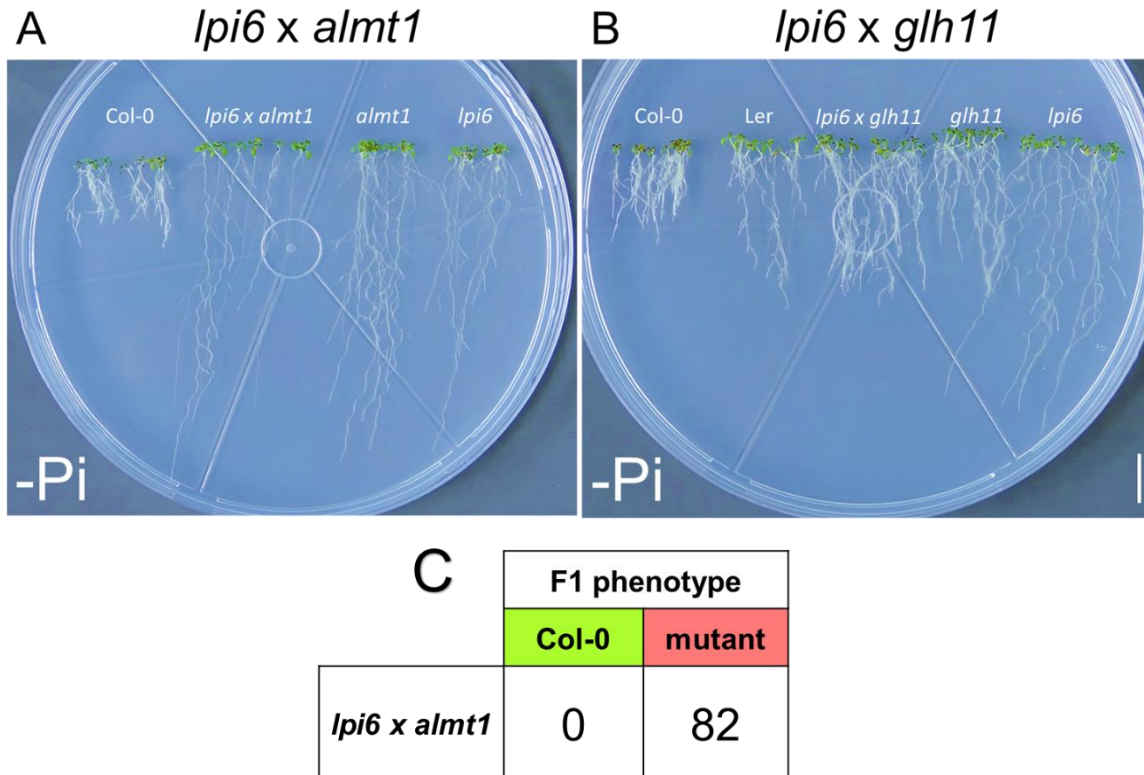


Figure 14. **Crosses with candidate genes revealed non-complementation between *lpi6* and *almt1* mutant lines of *Arabidopsis*.** (A) Seedlings of the F1 progeny of *lpi6* x *almt1* and *lpi6* x *glh11* crosses are shown (12 dag). As evidenced by the root architecture under -Pi conditions the *almt1* mutant was unable to complement *lpi6*. (B) Despite being in a Ler background, which inhibits primary root growth to a lesser extent than Col-0, *glh11* complemented the mutant phenotype as evidenced by the inhibition of primary root growth observed in comparison with *lpi6* mutants. (C) Mutant segregation rate of the *lpi6* x *almt1* cross. Scale bar equals 1 cm.

F1 progeny seedlings of the *lpi6* x *glh11* cross complemented each other which indicates that *glh11* possesses a functional copy of *LPI6* and thus is not the gene responsible

for the *lpi6* root phenotype under Pi deficiency conditions (Figure 14B). Moreover, *glh11* did not continue primary root elongation under -Pi conditions (Figure 14B). Surprisingly, *almt1* did show primary root growth inhibition in response to Pi deficiency conditions (Figure 14A). Such a phenotype has not been reported previously. Furthermore, the F1 progeny *lpi6* x *almt1* seedlings had a long primary root phenotype under Pi deficiency conditions (Figure 14A, C), which indicated non-complementation. Since *lpi6* is a recessive mutant this results indicates that *almt1* and *lpi6* are mutant alleles in the same gene.

To corroborate that *lpi6* was indeed an *almt1* EMS-induced mutant we amplified and sequenced *ALMT1* from Col-0 and *lpi6* genomic DNA (Figure 15). Sequencing results revealed a 13 base mutation (Figure 15A) in the 3rd exon of the At1g08430 locus that codes for ALMT1 (Figure 15B).

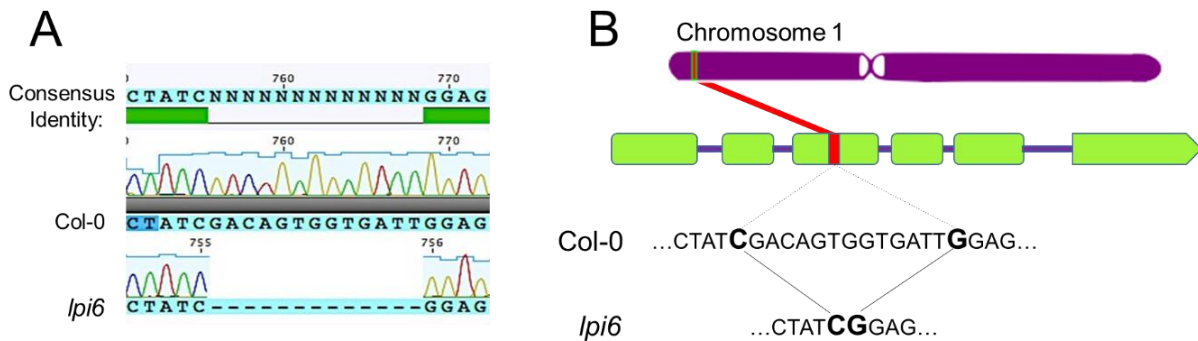


Figure 15. ***lpi6* presents a 13-base deletion inside the *ALMT1* locus.** (A) Electropherogram of the *lpi6* mutation. Sequencing results corroborated the 13-base deletion predicted by the genomic mapping of *lpi6*. (B) Schematic of the deletion predicted using mapping by sequencing methodology. As is depicted, a 13 base deletion is present in the 3rd exon of *ALMT1*.

The 13-base frameshifting deletion most likely produced the translation of an aberrant protein through the origination of a premature stop-codon. To test this, we analyzed the *ALMT1* reading frame that was generated after the deletion (Figure 16).

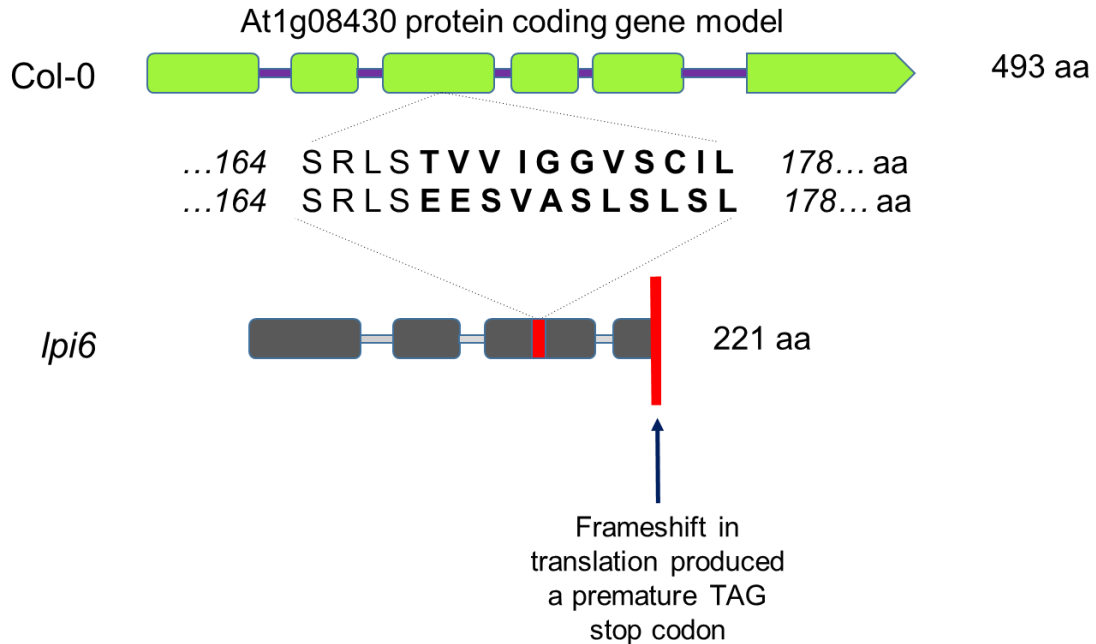


Figure 16. **Amino acid prediction of the *lpi6* aberrant protein produced by the 13-base deletion.** A premature stop codon is generated after the frameshift which causes the translation of an ALMT1 protein that has less than half the number of amino acids than its wild-type counterpart.

We predicted, by *in silico* sequence analysis, that the *lpi6* mutation produces a protein of 221 amino acids due to the generation of a premature TAG stop codon (Figure 16). Having less than half the amino acids of its wild-type counterpart, we speculate that the *lpi6* ALMT1 aberrant protein is most likely inactive and probably degraded by post-translational regulation mechanisms⁴⁴.

We then analyzed the classical local response to Pi starvation in *alm1* and *lpi6* seedlings (Figure 17). Phenotypically *lpi6* and *alm1* mutants showed the same phenotype under Pi deficiency conditions (Figure 17A, 17B). *lpi6* and *alm1* were concluded to have a statistically equal primary root length and number of lateral roots in Pi starvation as evidenced by a Tukey HSD analysis ($P < .05$) (Figure 17C, D).

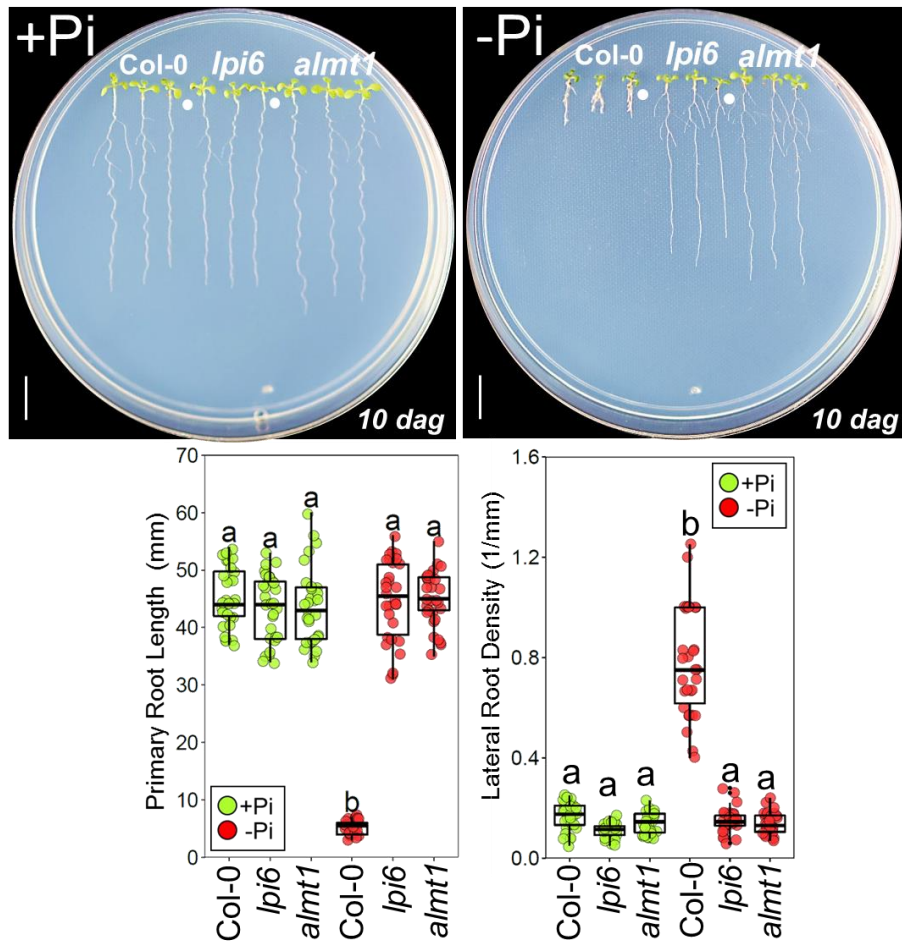


Figure 17. **Comparative root architecture response analysis of Col-0, *lpi6* and *almt1* seedlings grown under Pi deficiency conditions.** (A, B) Phenotypes of Col-0, *lpi6* and *almt1* 10 dag seedlings grown under +Pi (A) and -Pi (B) conditions. (C) Primary root length of Col-0, *lpi6* and *almt1* 10 dag seedlings grown under +Pi and -Pi conditions. (D) Lateral root density per mm of primary root of Col-0, *lpi6* and *almt1* 10 dag seedlings grown under +Pi and -Pi conditions. Green, red and blue dots depict Col-0, *lpi6* and *almt1* individuals (n=30 from 3 independent experiments), respectively. Statistical groups were determined using a Tukey HSD test (P-value < .05) and are indicated by letters.

Mapping by sequencing revealed a homozygous mutation in the *ALMT1* locus of *lpi6*, complementation analysis revealed the absence of root architectural response to Pi starvation in F1 seedlings of the *lpi6* x *almt1* cross. Sequencing of the *lpi6* At1g08430 locus corroborated the frameshift mutation that produces an aberrant, and most likely not

functional, ALMT1 protein. An analysis of the root architectural response to Pi starvation in *lpi6* and *almt1* seedlings revealed no statistical differences between the two mutant lines. Overall, mapping by sequencing studies show that a mutation in *ALMT1* is responsible for the *lpi6* under Pi deficiency conditions. Consequently, *lpi6* will be referred as *almt1* in the following sections of this work.

Analysis of *ALMT1* induction under Pi deficiency conditions

In order to analyze the expression of *ALMT1* in response to Pi deficiency conditions, a transgenic Col-0 line harboring the *proALMT1::GFP::GUS* construction was produced (see Materials and Methods). Confocal microscopy analysis of root tips (from the root cap to the start of the differentiation zone of the root) of the *proALMT1::GFP::GUS* reporter line revealed *ALMT1* expression to be induced by Pi starvation (Figure 18A). The upregulation of *ALMT1* under Pi deficiency conditions was corroborated by RT-PCR (qRT-PCR) analysis (Figure 18B). This upregulation under Pi deficiency condition supports a role of this gene in the Pi starvation response in *Arabidopsis thaliana*.

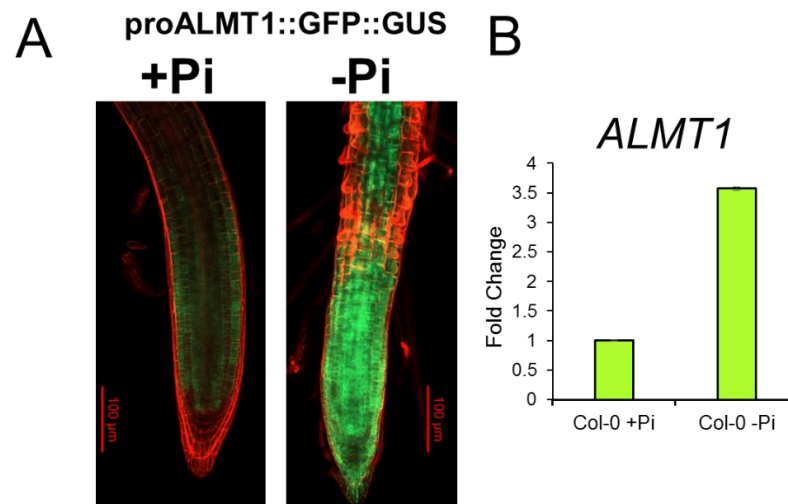


Figure 18. ***ALMT1* expression is induced under Pi starvation conditions.** (A) *ALMT1* expression was analyzed in root tips from Col-0 seedlings harboring the *proALMT1::GFP::GUS* construction 5 dag under -Pi and +Pi conditions. (B) qRT-PCR analysis (see Materials and Methods) of *ALMT1* expression under -Pi and +Pi conditions. *ALMT1* expression was analyzed in root tips of Col-0 seedlings grown under +Pi and -Pi conditions 5 dag.

Whole-transcriptome expression profiling of Col-0 and *almt1* root tips under Pi deficiency conditions.

The root tip plays a fundamental role in the plant's ability to sense and respond locally to Pi starvation³⁵, having isolated and identified a local response mutant we wanted to characterize the transcriptomic root tip response to Pi starvation in *almt1* and compare it to the wild-type (Col-0) response. Hence, we performed a whole transcriptome sequencing (RNA-seq) analysis of gene expression profiles of Col-0 and *almt1* root tips in response to Pi contrasting (-Pi/+Pi) conditions.

Seedlings were grown under +Pi and -Pi conditions and root tips from Col-0 and *almt1* individuals were dissected (5 dag) and total RNA extraction was performed. RNA-libraries were sequenced using the Illumina HiSeq platform, (further information about Illumina sequencing, data processing and statistical analyses is described in Materials and Methods). The four RNA-seq sample libraries used during our transcriptomic analysis are the following: Col-0 under +Pi conditions (Col-0+), Col-0 under -Pi conditions (Col-0-), *almt1* under +Pi conditions (*almt1*+) and *almt1* under -Pi conditions (*almt1*-). Library samples grouped under +Pi conditions but separated under -Pi conditions as evidenced by Multidimensional Scaling (MDS) analysis (Figure 19).

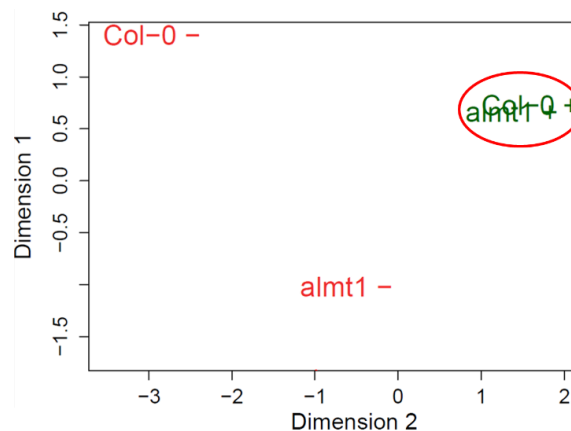


Figure 19. **MDS plot analysis of RNA-seq sample libraries.** Distance between samples (Col-0-, Col-0+, *almt1*-, *almt1*+) illustrate leading log fold change (logFC) differences between libraries.

We then performed pairwise comparisons to determine differential expression between samples (Col-0-/Col+; *almt1*-/*almt1*+). A total of 711 differentially expressed genes were found to be upregulated in Col-0 root tips subjected to -Pi conditions (Figure 20, Attachment 1) while only 174 genes were upregulated in *almt1* root tips (Figure 20, Attachment 1). A total of 346 genes were downregulated in Col-0 root tips while only 138 genes were downregulated in *almt1* in response to Pi deficiency conditions. (Figure 20, Attachment 1). A loss of transcriptional response to Pi starvation in *almt1* root tips was evidenced by the overall reduced number of up- and down-regulated transcripts in response to -Pi conditions and the loss of expression of the Col-0 differentially expressed genes in the insensitive mutant backgrounds (Figure 20).

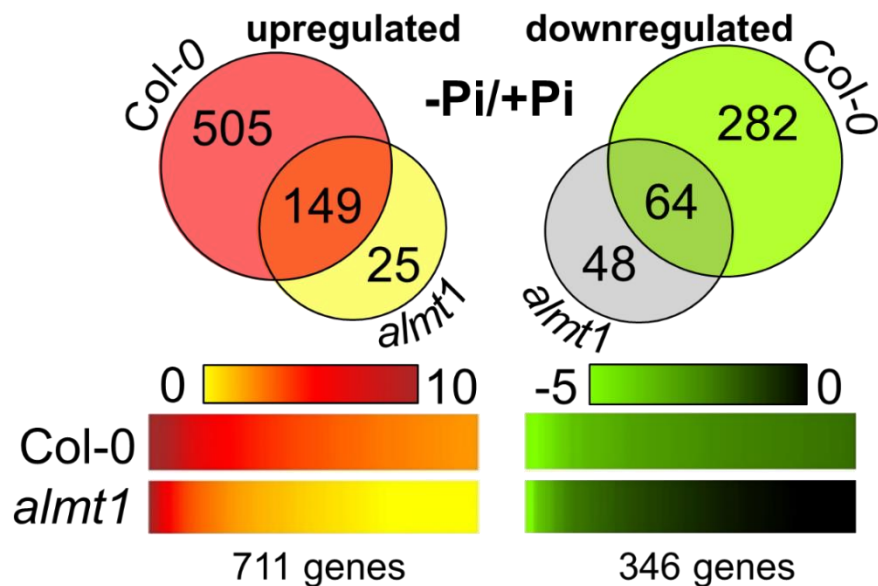


Figure 20. **A loss of transcriptional response in the root tips of *almt1* was evidenced by whole-genome transcriptome analysis.** Differential expression was assessed using a base two logarithm of the fold change (logFC) of transcript abundances resulting from pairwise comparisons (-Pi/+Pi) in root tips from Col-0 and *almt1* 5-day seedlings respectively. Differentially expressed genes were filtered using a logFC(-Pi/+Pi) > 2 threshold for upregulated transcripts, a logFC(-Pi/+Pi) < -2 threshold for downregulated transcripts and a false discovery rate value (FDR) < 0.0005. A Venn diagram of unique and shared up- and down-regulated transcripts in response to -Pi/+Pi conditions. Differential expression distributions of the Col-0 -Pi/+Pi responsive genes in *stop1* and *almt1* root tips.

Distributions illustrate genes sorted in a higher to lower expression fashion based on the logFC(-Pi/+Pi) values of the differentially expressed genes for each of the three genetic backgrounds.

One hundred and forty nine genes were upregulated in Col-0 and *almt1* root tips in response to Pi deficiency conditions, so we performed a Gene Ontology (GO) analysis of the commonly induced transcripts (Figure 21):

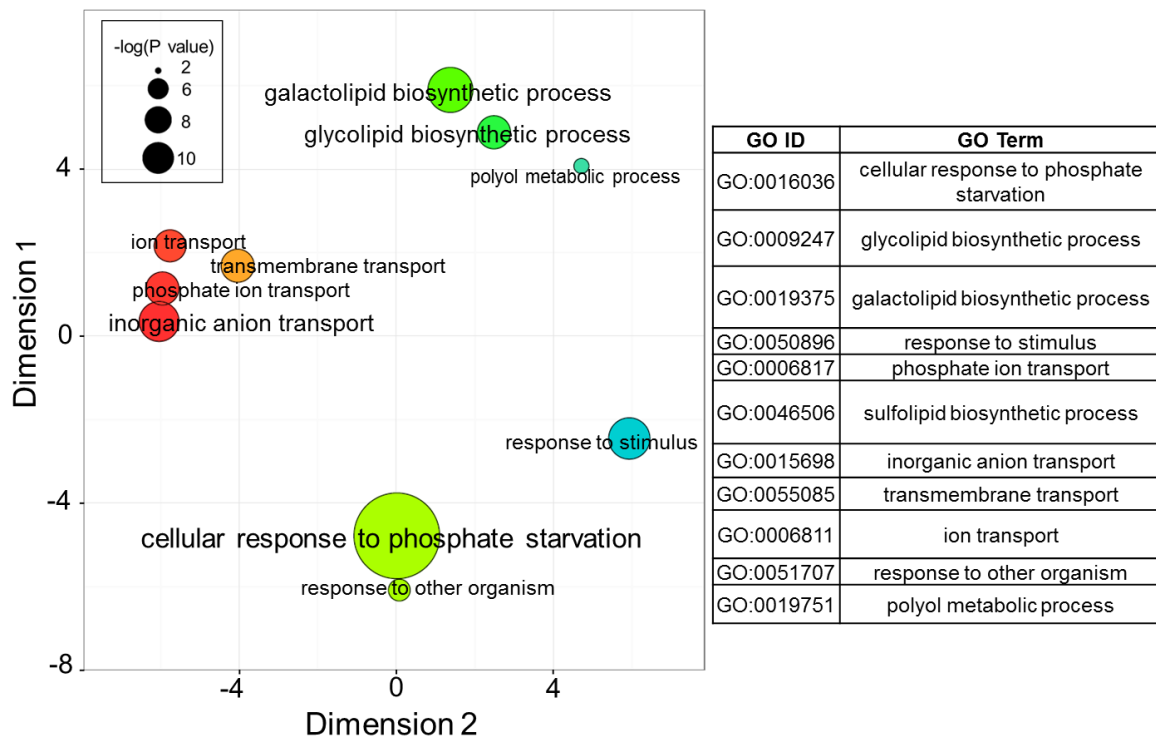


Figure 21. **Gene Ontology analysis of the upregulated transcripts in Col-0 and *almt1* root tips revealed induction of the phosphate starvation response in both backgrounds.** Multidimensional scaling bubble plot of GO terms. Bubble sizes are proportional to the $-\log(P\text{-value})$ of over-representation, thus bigger bubbles represent the more significantly overrepresented categories. Corresponding GO ID and Terms are listed in the table (right).

Over-represented categories in the shared upregulated transcripts included the cellular response to phosphate starvation, glycol- and galactolipid biosynthetic process, phosphate ion transport categories (Figure 21). Such categories encompass systemic PSR genes such as *SPX1-3*, *PLDZ2*, *MGDG2-3*, *PHT2*, *PHT5*, *RNS1* that were induced in both

Col-0 and *alm1* root tips in response to Pi starvation conditions. Thus, we hypothesized that the transcriptional PSR response was similarly upregulated in Col-0 and *alm1* root tips. To test this, we looked at the logFC values of systemic PSR genes known to be systemically upregulated by the master regulator PHR1^{1,3,4} (Figure 22).

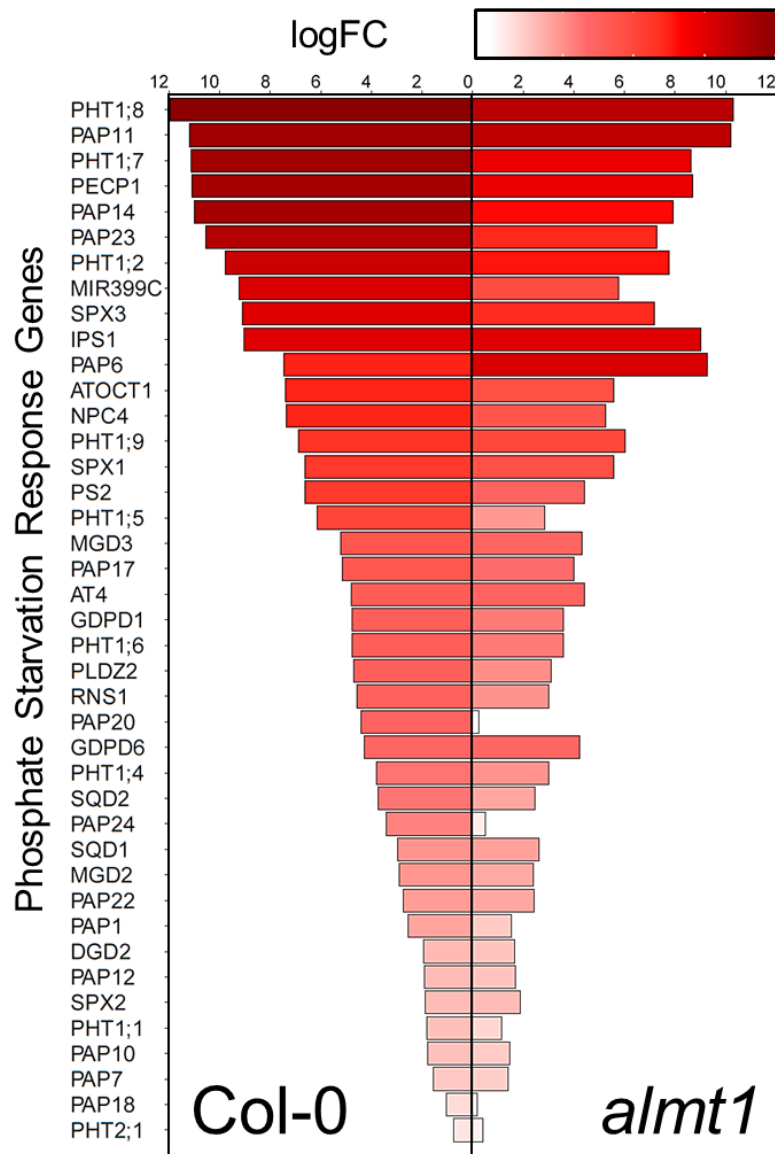


Figure 22. **Phosphate starvation response genes are induced in a similar fashion in Col-0 and *alm1* root tips.** Bars depict the respective gene logFC in Col-0 and *alm1* root tips in response to Pi deficiency conditions. Bar color also depicts logFC, color gradient is indicated in the key.

In spite of the fact that some of the transcripts showed lower levels of induction, a similar transcriptomic response of PSR genes was observed for both the WT and *lpi6*. Such tendency was evidenced by the logFC values of the PSR genes in Col-0 and *almt1* root tips. GO analysis and a specific analysis of the expression of systemically induced PSR genes revealed that the systemic response to Pi starvation is still active in the *almt1* mutant.

We then analyzed what kind of processes were induced in Col-0, but not in *almt1* root tips, such processes ultimately would be the responsible for the contrasting root phenotypes of Col-0 and *almt1* seedlings under Pi deficiency conditions. Thus, we performed a GO analysis of the 505 unique upregulated transcripts in Col-0 seedlings (Figure 23).

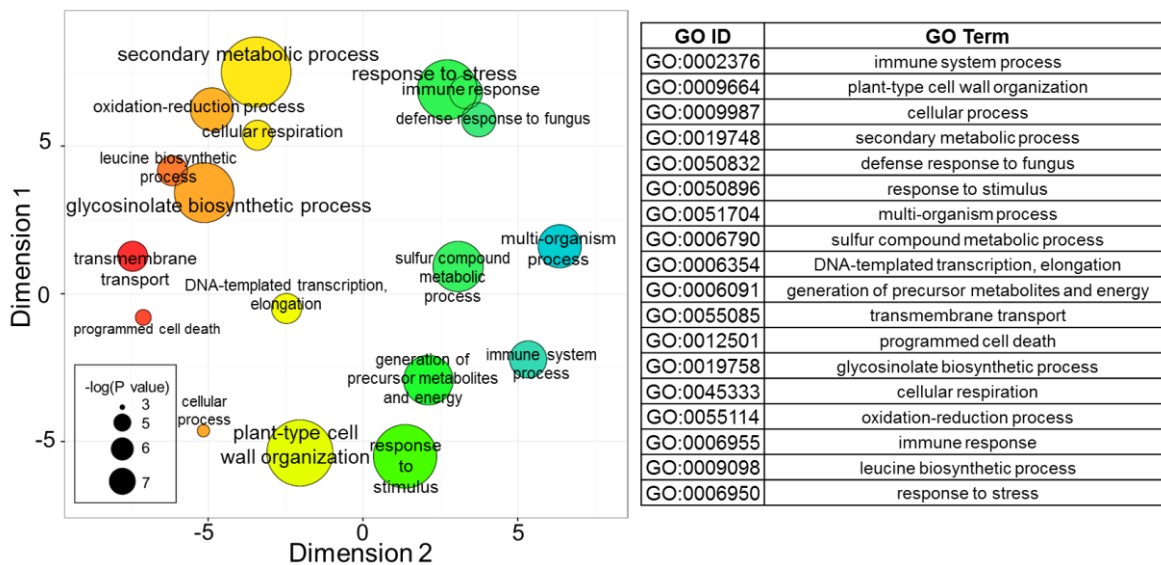


Figure 23. **GO analysis of the unique upregulated transcripts in Col-0 root tips revealed cell wall related processes to be over-represented.** Multidimensional scaling bubble plot of GO terms. Bubble sizes are proportional to the $-\log(P\text{-value})$ of over-representation, thus bigger bubbles represent the more significantly overrepresented categories. Corresponding GO ID and Terms are listed in the table (right).

The secondary metabolic processes (GO:0019748) category, that includes genes of the lignin biosynthetic pathway⁴⁵, and the plant-type cell wall organization (GO:0009664) category, which includes expansin-like proteins and peroxidases^{46,47}, were overrepresented in Col-0 uniquely upregulated transcripts. (Figure 23). Other intriguing categories such as

the glucosinolate biosynthetic process (GO:0019758) and other biotic-stress related categories (GO:0050832, GO:0006955, GO:0051704) were also found to be upregulated in the Col-0 background and absent in *alm1*.

GO analysis revealed that cell-wall related processes, which have been linked recently to the local response to Pi starvation^{48,49}, were absent in the insensitive background. So, we analyzed the logFC of cell-wall related transcripts in response to Pi deficiency conditions in Col-0 and *alm1* root tips (Table 2).

		logFC (-/+)					
		ID	Col-0	<i>almt1</i>	Description	Graph Number	
LOCAL RESPONSE	CELL-WALL MODIFYING ENZYMES	LIGNIN METABOLISM	AT1G67980	7.34	-1.24	S-ADENOSYL-L-METHIONINE TRANSCAFFEYOYL COENZYME A 3-O-METHYLTRANSFERASE (CCoAOMT)	36
			AT4G37970	2.07	-0.99	CINNAMYL ALCOHOL DEHYDROGENASE 6 (CAD6)	37
			AT1G77520	2.95	0.42	O-METHYLTRANSFERASE FAMILY PROTEIN	38
			AT1G33030	3.93	0.10	O-METHYLTRANSFERASE FAMILY PROTEIN	39
			AT5G05390	10.37	1.41	LACCASE FAMILY PROTEIN (LAC12)	40
		PLANT-TYPE CELL WALL ORGANIZATION	AT1G12040	2.98	0.35	LEUCINE-RICH REPEAT/EXTENSIN 1 (LRX1)	41
			AT1G21310	2.24	0.09	EXTENSIN 3 (EXT3)	42
			AT1G23720	2.50	-0.33	EXT-LIKE FAMILY PROTEIN	43
			AT1G26250	2.71	-5.64	EXT-LIKE FAMILY PROTEIN	44
			AT1G61080	2.61	0.56	HYDROXYPROLINE-RICH FAMILY PROTEIN	45
			AT1G62440	2.45	0.56	LEUCINE-RICH REPEAT/EXTENSIN 2 (LRX2)	46
			AT1G64670	3.25	1.07	BODYGUARD1 (BDG1); ALPHA BETA HYDROLASE ACTIVITY.	47
			AT1G69530	3.92	1.62	EXPANSIN A1 (EXPA1)	48
			AT1G76930	3.12	-0.08	EXTENSIN 4 (EXT4)	49
			AT2G16630	5.60	0.90	EXTENSIN-LIKE FAMILY PROTEIN	50
			AT2G18660	9.70	5.38	EXTENSIN-LIKE FAMILY PROTEIN	51
			AT2G24980	3.84	0.24	EXTENSIN 6 (EXT6)	52
			AT2G26440	2.73	-0.18	PECTIN-METHYLESTERASE INHIBITOR SUPERFAMILY	53
			AT2G37640	2.19	0.49	EXPANSIN 3 (EXP3)	54
			AT2G43150	2.14	-0.55	EXTENSIN-LIKE FAMILY PROTEIN	55
			AT3G09405	3.97	1.43	EXTENSIN-LIKE FAMILY PROTEIN	56
			AT3G15370	4.37	-0.17	EXPANSIN 12 (EXPA12)	57
			AT3G28550	3.50	-0.06	EXTENSIN-LIKE FAMILY PROTEIN	58
			AT3G29810	2.12	-0.29	COBRA-LIKE PROTEIN 2 PRECURSOR (COBL2)	59
			AT3G45960	3.50	0.28	EXPANSIN-LIKE A3 (EXLA3)	60
			AT3G54580	4.01	-0.08	EXTENSIN-LIKE FAMILY PROTEIN	61
			AT3G54590	3.91	0.04	HYDROXYPROLINE-RICH GLYCOPROTEIN (HRGP1)	62
			AT4G02330	4.77	-0.78	PECTIN-METHYLESTERASE (ATPMEPCRB)	63
			AT4G08400	2.76	-0.04	EXTENSIN-LIKE FAMILY PROTEIN	64
			AT4G08410	2.73	-0.22	EXTENSIN-LIKE FAMILY PROTEIN	65
			AT4G13390	2.50	-0.13	EXTENSIN 12 (EXT12)	66
			AT4G38770	3.20	-0.90	PROLINE-RICH FAMILY PROTEIN	67
			AT5G06630	3.49	0.37	EXTENSIN-LIKE FAMILY PROTEIN	68
			AT5G06640	3.82	0.12	EXTENSIN 10 (EXT10)	69
			AT5G06860	2.46	1.05	POLYGALACTURONASE INHIBITING PROTEIN 1 (PGIP1)	70
			AT5G06870	4.19	3.55	POLYGALACTURONASE INHIBITING PROTEIN 2 (PGIP2)	71
			AT5G35190	2.52	0.24	EXTENSIN 13 (EXT13)	72
			AT5G48070	2.64	0.96	XYLOGLUCAN ENDOTRANSGLUCOSYLASE/HYDROLASE 20 (XTH20)	73
			AT5G49080	3.32	0.26	EXTENSIN 11 (EXT11)	74
			PEROXIDASES	AT2G18150	8.22	3.13	PEROXIDASE SUPERFAMILY PROTEIN
		AT2G41480		2.22	-0.24	PEXOXIDASE SUPERFAMILY PROTEIN	76
		AT3G49110		4.99	0.42	PEROXIDASE CA (PRXCA) CIII	77
		AT3G49120		2.09	1.30	PEROXIDASE CB (PRXCB) CIII	78
		AT4G08770		3.27	0.45	PEROXIDASE 37 (Prx37)	79
		AT4G08780		5.90	-0.73	PEROXIDASE SUPERFAMILY PROTEIN	80
		AT4G36430		7.99	2.73	PEROXIDASE SUPERFAMILY PROTEIN	81
		AT5G05340		13.42	0.86	PEROXIDASE 52 (PRX52)	82
		AT5G06720		5.44	-1.04	PEROXIDASE 2 (PA2)	83
		AT5G06730		4.41	0.35	PEROXIDASE SUPERFAMILY PROTEIN	84
		AT5G19880		4.52	1.90	PEROXIDASE SUPERFAMILY PROTEIN	85
		AT5G39580		4.13	1.09	PEROXIDASE SUPERFAMILY PROTEIN	86
		AT5G47000		3.02	-0.69	PEROXIDASE SUPERFAMILY PROTEIN	87

Table 2. Comparison of Col-0 and *almt1* differential expression values revealed a downgrade of cell-wall related regulation in *almt1* in response to Pi deficiency conditions. The expression of lignin metabolism genes⁴⁵, plant-type cell wall organization genes from the GO:0009664 category and cell wall peroxidases genes was analyzed. LogFC(-/+) resulting of the pairwise comparison of samples are shown. A red colored logFC cell value depicts a differentially expressed transcript in the respective background.

We observed that lignin metabolism was upregulated in Col-0 and downregulated in *alm1* root tips, so we performed phloroglucinol lignin staining of Col-0 and *alm1* root tips (Figure 23B).

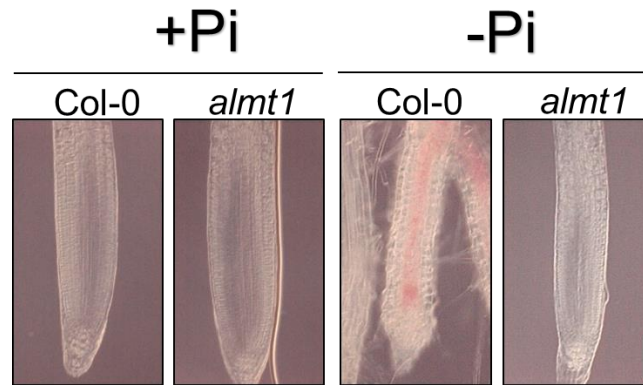


Figure 23B. **Lignin deposition is absent in the roots of *alm1* mutants.** Lignin presence is depicted by red color staining. Phloroglucinol lignin staining was performed on the roots of 5 day Col-0 and *alm1* seedlings grown under Pi deficiency conditions. Scale bar equals 100 μ m.

Our transcriptomic data predicted the upregulation of lignin deposition in Col-0 root tips and the downregulation of the same process in *alm1* root tips under Pi deficiency conditions. Lignin staining (Figure 23B) confirmed such results and revealed the presences of lignin deposition in the root tips of Col-0 seedlings. An absence of lignin deposition in Pi starved roots of *alm1* seedlings.

We then analyzed the overrepresented GO terms of the downregulated transcripts in Col-0 and *alm1* root tips. We did not find any over-represented term in our GO analysis of the shared and unique genes of *alm1* downregulated transcripts. In the case of the unique downregulated transcripts in Col-0 root tips, we found two over-represented biological process categories: water transport (GO:0006833) and photosynthesis (GO:0015979), both processes have already been reported to be downregulated in *Arabidopsis* in response to Pi deficiency conditions^{50,51}.

A local vs systemic regulation analysis that compares the expression of the PSR genes presented in Figure 22 and the cell-wall modifying enzymes presented in Table 2, is presented in Figure 24.

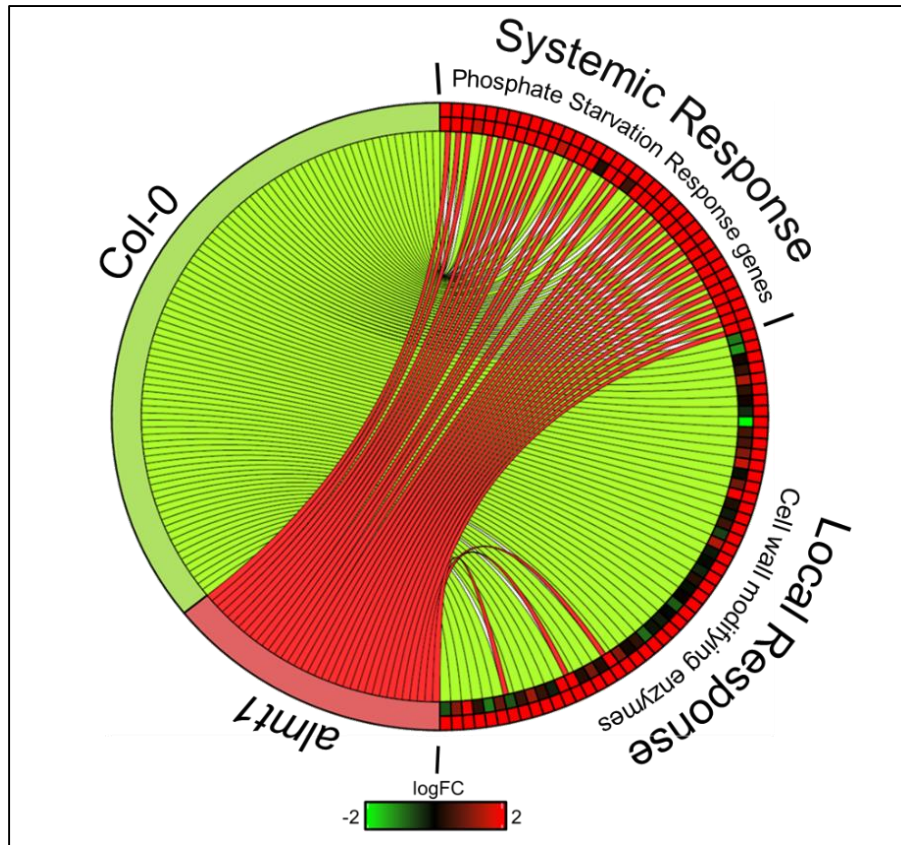


Figure 24 (last page). **Differential expression analysis of local and systemic regulation in Col-0 and *almt1* root tips.** Graph illustrates a heatmap (right) of the logFC(-Pi/+Pi) values of phosphate starvation response genes and transcripts of cell wall modifying enzymes. Connections between genes in the heatmap (left) and genotypes Col-0 and *almt1* (right) depict a differentially expressed gene in the respective genotype. Differentially expressed genes that conform the systemic and local transcriptional response to Pi starvation are listed in Figure 19 and Table 2 and are all listed in Attachment 2.

Overall, RNA-seq analysis revealed that the systemic response to Pi starvation is active in both Col-0 and *almt1* root tips, whereas upregulation of cell wall related processes, which has been recently shown to be absent in local response mutants^{48,49}, was found to be active in the Col-0 background and lost in the root tips of our *almt1*. Whole-genome sequencing revealed a previously unreported role of *ALMT1* in the transcriptomic regulation of the local response to Pi starvation in *Arabidopsis thaliana*.

The *alm1* mutant phenotype under Pi deficiency conditions can be rescued by external malate addition.

Next, we wanted to determine the role of malate secretion under Pi deficiency conditions. In order to do so we supplemented the medium with different concentrations of malic acid to see if it had any effect on primary root elongation of *alm1* under Pi-deficiency conditions (Figure 25). A reversibility of the mutant phenotype was observed as the malate concentration in the medium was increased (Figure 25).

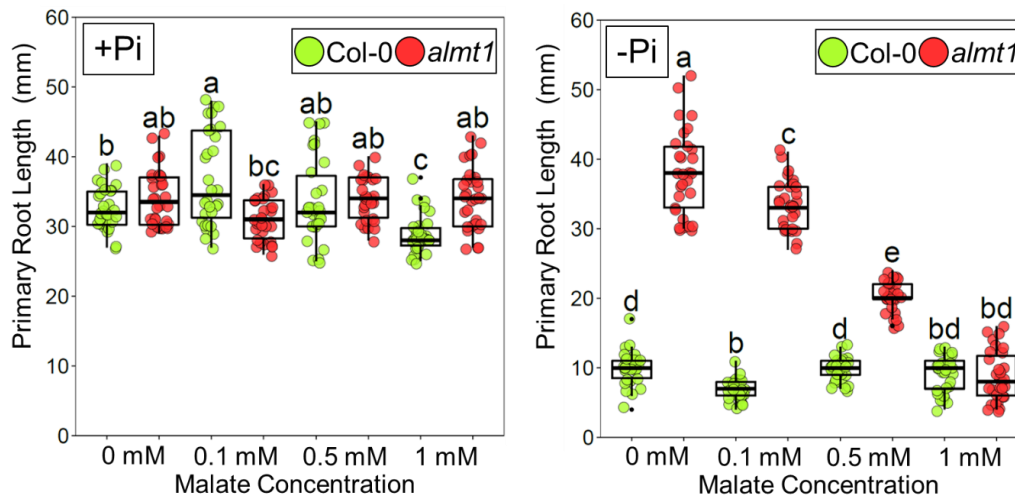


Figure 25. **Malate supplementation of the medium revealed the reversibility of the *alm1* mutant.** Increasing concentrations of malic acid were supplied to the culture medium (+Pi/-Pi). At 1 mM malate, *alm1* primary root growth inhibition under Pi deficiency conditions was complete and similar to that observed for the WT with or without the malate treatment. Green and red dots represent Col-0 and *alm1* individuals (n=30 from 3 independent experiments), respectively. Statistical groups were determined using a Tukey HSD test (P-value < .05) and are indicated by letters.

Malic and citric acids have been reported to be the major organic acids secreted by plants under Pi starvation conditions⁵²⁻⁵⁴. Therefore, we supplemented the medium with citrate to observe if the reversion of the mutant phenotype was an exclusive phenomenon of malate supplementation (Figure 26).

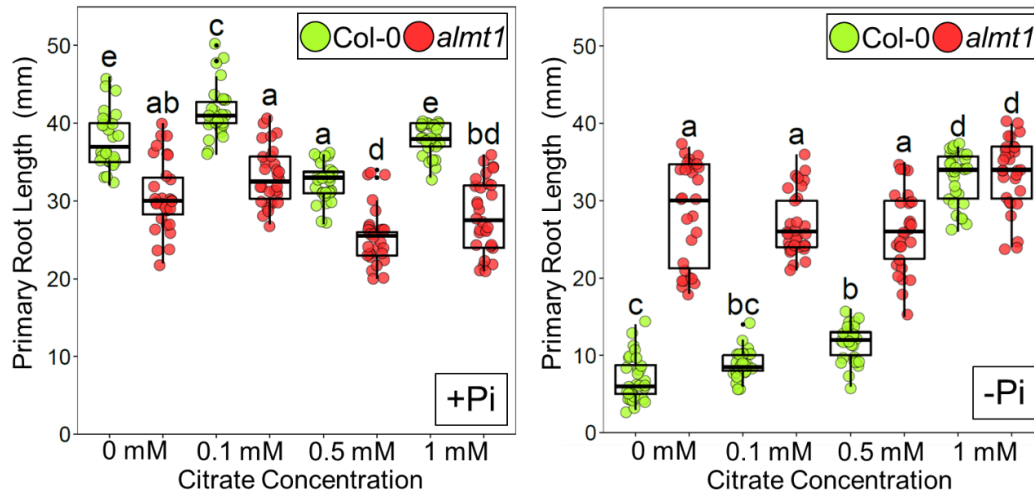


Figure 26 (last page). **Citrate supplementation of the medium revealed the reversibility of the *almt1* mutant.** Increasing concentrations of citric acid were supplied to the culture medium (+Pi/-Pi). At 1 mM citrate, primary root length evidenced primary root inhibition of the *almt1* under Pi deficiency conditions. Green and red dots represent Col-0 and *almt1* individuals (n=30 from 3 independent experiments), respectively. Statistical groups were determined using a Tukey HSD test (P-value < .05) and are indicated by letters.

Citrate did not complement *almt1* as evidenced by primary root length of the *almt1* seedlings at 1 mM citrate supplementation of the medium. Surprisingly, citrate abolished Col-0 primary root inhibition under Pi deficiency conditions (Figure 26). A possible explanation for this is found the involvement of citrate in iron-transport^{55,56}, an *Arabidopsis* mutant defective in a citrate transporter (*frd3*) has been reported to have an hypersensitive phenotype in response to Pi deficiency conditions^{37,55}. Although citrate supplementation revealed an interesting Col-0 phenotype, the reversibility of the *almt1* phenotype was concluded to be a specific phenomenon of malate supplementation.

At 1 mM malate supplementation (+M) conditions a complete reversibility of the aberrant *almt1* primary root phenotype in *almt1* was observed (Figure 26). So, we performed a characterization of root architectural traits to assess the reversibility of the *almt1* phenotype under Pi deficiency conditions (Figure 27).

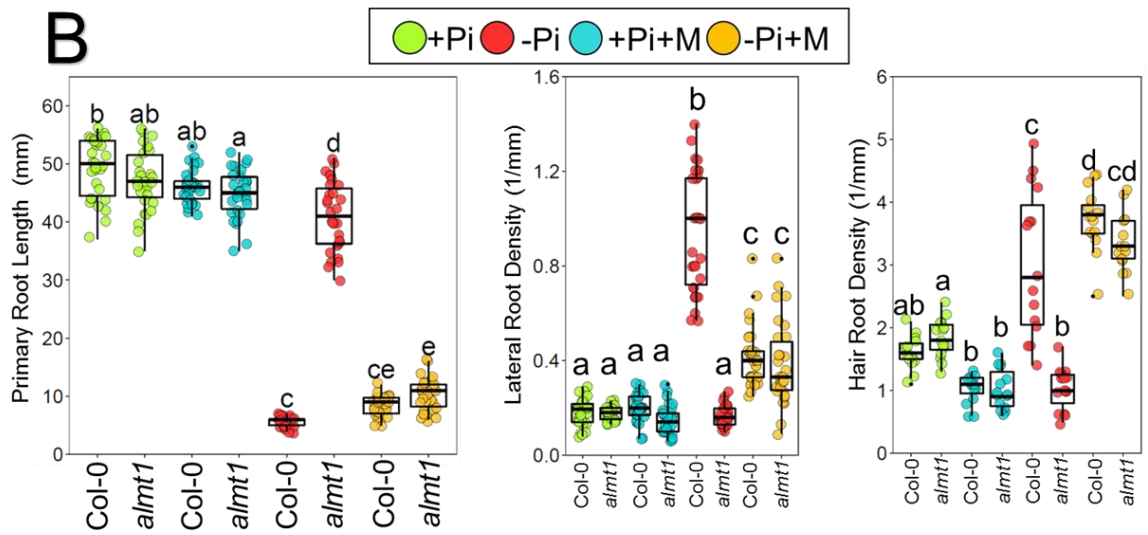
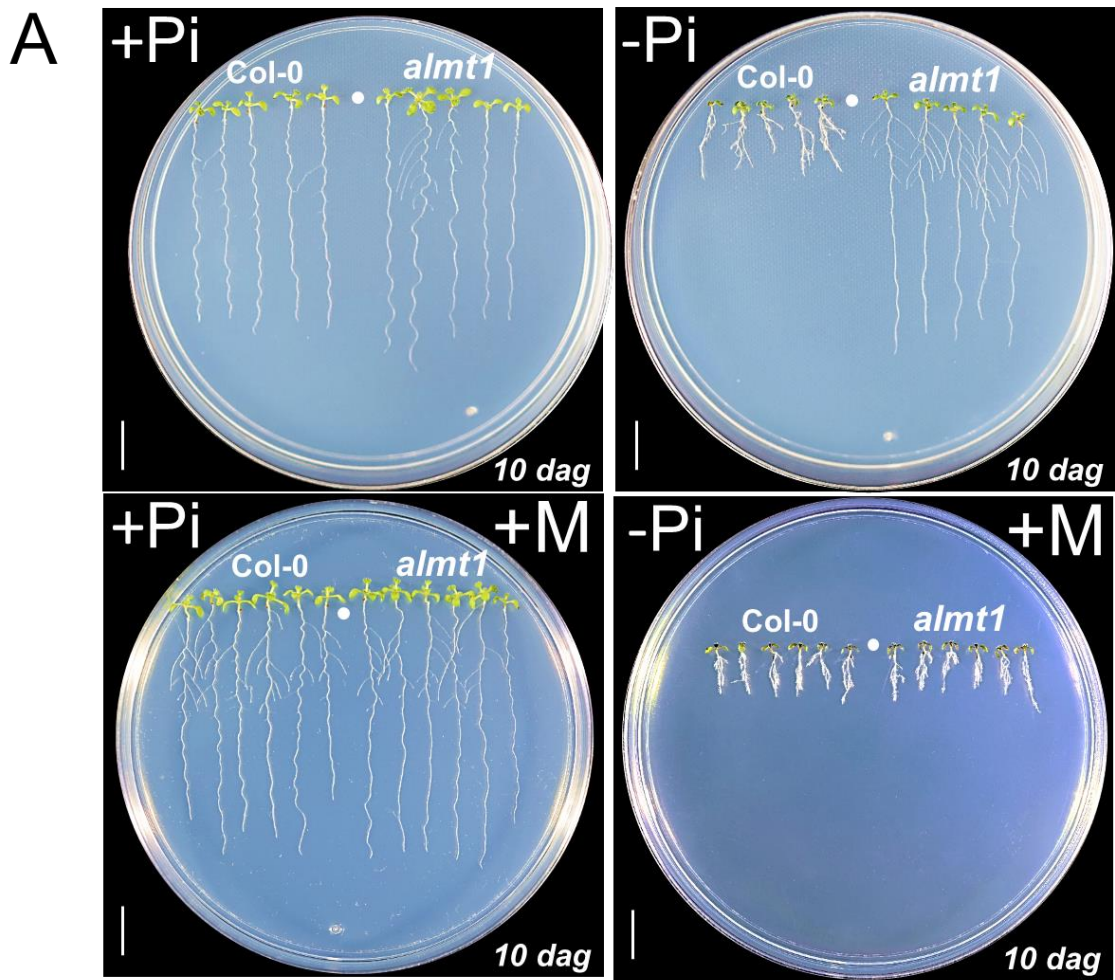


Figure 27 (last page). **1 mM Malate supplementation of the medium rescued the *almt1* mutant phenotype under Pi deficiency conditions.** (A) Phenotypes of Col-0 and *almt1* seedlings under +Pi +M(1mM) and -Pi +M(1 Mm) conditions 10 dag. Phenotypes of Col-0 and *almt1* seedlings under +Pi and -Pi conditions shown in figure 10 are shown for comparative purposes (B) Root architectural response of Col-0 and *almt1* seedlings. Dots represent Col-0 and *almt1* individuals (n=30 from 3 independent experiments). Conditions are indicated by colors. Statistical groups were determined using a Tukey HSD test (P-value < .05) and are indicated by letters. Scale bar equals 1 cm.

No effects of malate were observed under control conditions (+Pi+M) as evidenced by phenotype and root architecture analysis (Figure 27A, B). The similar inhibition of primary root growth under -Pi+M conditions was evidenced along with an increase in lateral root number and root hair density (Figure 27B) confirming the rescuing of the mutant phenotype. This suggested a role of malate in the regulation of root architecture under Pi deficiency conditions.

The malate-dependent iron-distribution mechanism that occurs in *Arabidopsis thaliana* in response to Pi starvation conditions

Iron distribution has been reported to be affected in mutants of the local response to Pi starvation¹³, thus, we analyzed iron distribution in Col-0 and *almt1* root tips using Perls-DAB iron staining^{13,57} (Figure 28). Under +Pi conditions, root tips from Col-0 and *almt1* seedlings showed similar patterns of iron distribution (Figure 28). An increased Fe-staining was observed in the root tips of Col-0 seedlings under Pi deficiency conditions. Such iron distribution was not observed in the root tips of *almt1* seedlings which showed a lower intensity of Fe-staining under -Pi conditions (Figure 28).

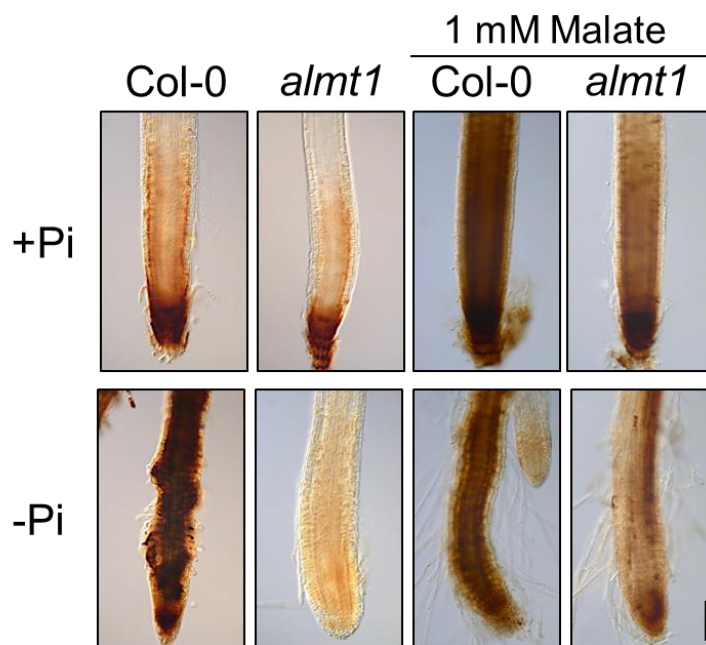


Figure 28. **Iron distribution under Pi deficiency conditions is affected in the root tips of the local response mutant *almt1*.** DAB-Perls (Perls, 3'3-diaminobenzidine) iron staining of 10-day root tips from Col-0 and *almt1* seedlings grown under the indicated conditions. Brown color intensity indicates the presence of reactive oxygen species (ROS) which is concomitant with iron distribution. Scale bar equals 100 μ m.

Fe-staining in the root tips of the insensitive lines under -Pi conditions was observed to be even less intense than Fe-staining in the root tips of insensitive lines seedlings grown under +Pi conditions (Figure 28). Malate supplementation of the medium enhanced iron accumulation in the root of Col-0 and *almt1* seedlings regardless of Pi conditions, iron accumulation in the primary roots of *almt1* was observed *under -Pi+M* conditions (Figure 28). While the iron distribution of roots from malate-supplemented *almt1* seedlings was not observed to be exactly like Col-0 plants under Pi deficiency conditions a more similar iron distribution was observed.

Iron uptake through *IRT1* (Vert et al. 2002) has been reported to be transcriptionally downregulated under Pi deficiency condition (Hoehenwarter et al. 2016), *IRT1* repression suggests an inhibition of Pi uptake which could contribute to extracellular iron accumulation. The multicopper oxidase *LPR1* has been reported to act as a cell-wall ferroxidase in an iron-dependent RAM-exhaustion mechanism in *Arabidopsis*¹³. *IRT1* and *LPR1* were not

differentially expressed in Col-0 in response to Pi deficiency conditions according to our RNA-seq data. So we performed a qRT-PCR analysis of the *LPR1* relative levels of expression in the root tips of Col-0 and *alm1* mutants (Figure 29).

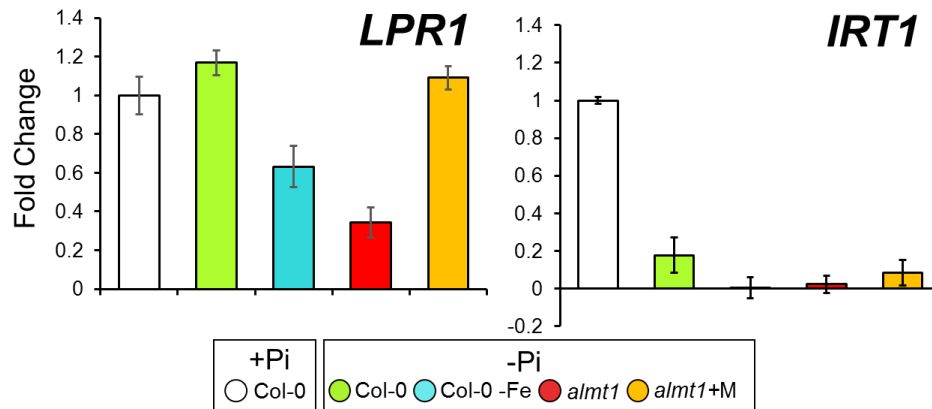


Figure 29. ***LPR1* and *IRT1* relative levels of expression in Col-0 and *alm1* root tips under iron-deficiency and malate supplementation, respectively.** qRT-PCR analysis (see Materials and Methods) of *LPR1*, *IRT1* expression under Pi deficiency conditions (-Pi) iron and phosphate deficiency conditions (-Fe) and Pi deficiency and 1 mM supplementation (+M) conditions. Expression levels were normalized using Col-0 +Pi levels of expression (represented by 1) as a reference for all samples.

Col-0 continues primary root growth when it is grown under both iron and phosphate deficiency conditions³⁷ (Pi -Fe). The *LPR1* level of expression was downregulated in Col-0 under -Pi -Fe conditions and in the *alm1* mutant under -Pi deficiency conditions, which correlates with an absence of RAM exhaustion. Interestingly, *LPR1* induction correlated with RAM exhaustion as it is upregulated in Col-0 under Pi-deficiency conditions and *alm1* under -Pi+M conditions. *IRT1* was downregulated regardless of genotype and/or condition.

Overall, iron distribution under Pi deficiency conditions is complemented in *alm1* root tips by malate supplementation of the medium. Studies of *LPR1* relative expression reveal an induction of the multicopper-oxidase under Pi deficiency conditions. A downregulation of *LPR1* expression was observed to be concomitant with long root phenotypes under Pi

deficiency conditions. *LPR1* levels of expression and root inhibition under Pi deficiency conditions, were restored in *alm1* mutants by malate supplementation. *IRT1* expression was downregulated in Col-0 and *alm1* under Pi deficiency conditions. Our iron distribution and qRT-PCR studies suggest an involvement of *ALMT1* in iron distribution in the root and in the induction of the expression of *LPR1*, and thus, a malate-dependency of the iron-distribution mechanism that triggers RAM exhaustion in *Arabidopsis thaliana*.

DISCUSSION

low phosphate insensitive 6, a mutant line that continued primary root growth under Pi-deficiency conditions, was isolated through a screening of EMS-mutagenized seeds under Pi deficiency conditions in our lab (Mora, J. *unpublished*). Through whole-genome mapping by sequencing techniques we were able to identify *ALMT1* as the mutated locus in *lpi6*. *ALMT1* has been reported to be one of the key players of a malate efflux mechanism that is induced under Aluminum stress conditions in *Arabidopsis*^{11,12}.

Analysis of QC identity and cell cycle markers revealed that RAM activity is maintained in the primary root of *alm1* under Pi-deficiency conditions. The modifications of root system architecture which are preceded by RAM-exhaustion in *Arabidopsis*⁵, enhance the soil exploration area of the root and contribute to the improvement of Pi uptake^{8,9,19}. Carboxylate secretion into the soil has been reported to have an involvement in regulating physiological processes such as the regulation of primary root growth under aluminum stress conditions^{58,90}. Thus, while the mutant phenotype of *alm1* under Pi deficiency conditions resembles an unstressed plant it is most likely not a convenient trait for a plant when facing Pi challenging conditions as it cannot alter its root architecture in response to stress conditions which could compromise its ability to adapt to its environment.

Analysis of *proALMT1::GUS::GFP* transgenic lines revealed *ALMT1* expression to be induced in the root tip, a root region that is essential for Pi sensing^{35,36}. *ALMT1* induction was observed in the root cap of *proALMT1::GUS::GFP* plants under -Pi conditions, this was not observed under +Pi conditions. This was interesting as it has been reported that up to a 20% of the plant's total Pi uptake is performed through the root cap⁵⁹. This indicates that

ALMT1 could play an additional role in phosphate nutrition besides regulating root morphology in response to Pi deficiency conditions.

Whole-genome transcriptomic analysis revealed that the malate-efflux gene *ALMT1* to be essential for the transcriptomic regulation of over 500 transcripts that are differentially expressed in the root tips of Col-0 roots and are under-regulated in *almt1* root tips. An upregulation of the PSR genes that comprehend the PHR1-dependent systemic response to Pi starvation²⁻⁴ was observed in the root tips of the two analyzed genetic backgrounds. Cell-wall related transcripts of the lignin metabolism⁴⁵, extensin- and expansin-like proteins^{60,61} and peroxidases^{47,62} were under-regulated in the root tips of *almt1*, this in agreement with the results of a transcriptomic study and a metabolite profiling of the local response to Pi starvation mutants *lpr1* and *pdr2*^{48,49} in which cell-wall related processes were also found to be downregulated.

Lignin deposition was present in Col-0 root tips and absent in *almt1* root tips under Pi deficiency conditions. *LPR1* is a member of the laccase (polyphenol oxidase) family of proteins¹³ that catalyze the polymerization of lignin subunits⁴⁹. *LPR1* expression was upregulated in Col-0 and downregulated in the *almt1* background under Pi deficiency conditions. Peroxidases were also observed to be upregulated in Col-0 and downregulated in *almt1* root tips in response to -Pi conditions. The lignification process is catalyzed by laccases and peroxidases⁹¹ and has been reported to be downregulated in rapidly growing tissues of *Oryza sativa*⁹². Peroxidase-catalyzed lignification has been reported to decrease cell wall plasticity causing the inhibition of cell growth as a consequence⁹³⁻⁹⁵. Lignin deposition has also been reported to limit the efflux of metals from the vasculature system into the shoot⁹⁶. Lignin deposition could contribute to the inhibition of cell growth and iron accumulation in the root under Pi deficiency conditions leading to the initiation of the iron-dependent RAM exhaustion program^{13,23}.

Being able to chelate metals, carboxylate-iron complexes have been closely related with iron uptake⁶³ and transport^{55,56}. The *FERRIC REDUCTASE DEFECTIVE 3* (*FRD3*) gene that encodes for a citrate transporter has been related to iron uptake and Pi deficiency

in *Arabidopsis*³⁷. It has been reported that *frd3* seedlings hyper-accumulate iron in the root and to have increased local response to Pi starvation³⁷. Most of the catalyzed reactions by the cell-wall related enzymes that were found to be upregulated and under-regulated in response to Pi deficiency conditions in *almt1* root tips require or involve iron ions^{45,47,60–62,64}. This is in congruence with an iron-dependency of the root response to Pi starvation that has been reported in *Arabidopsis*³⁷. Callose deposition in the root stem cell niche was also reported to be an iron-dependent mechanism and related to RAM-exhaustion¹³. Iron-distribution and the downgrade of cell-wall deposition enzymes in the root tips of *almt1* seedling suggests that the function of ALMT1 in response to Pi-starvation is to excrete malate, a phenomenon that is essential for iron uptake, and acts upstream of the *LPR1* and *PDR2* genetic regulation network, which in turn orchestrates *Arabidopsis* RAM-exhaustion³⁶.

Malate supplementation of the media rescued the *almt1* mutant phenotype under Pi deficiency conditions in a dose-dependent manner. This suggests a role of malate in the regulation of primary root growth under Pi deficiency conditions, as the *almt1* mutation can be complemented by supplementation of the organic acid in the medium. Being able to form complexes with iron that can be transported⁶⁵, external malate has the ability to modify iron-distribution in the RAM as evidenced by iron staining. RAM-exhaustion can be triggered in *almt1* mutants under Pi deficiency conditions by the supplementation of malate in the culture medium which evidences a direct role of malic acid in the iron-dependent regulation of RAM-exhaustion under Pi deficiency conditions.

A downregulation of *IRT1* transcripts under Pi deficiency conditions has been observed in our qRT-PCR studies and previous evidence^{48, 66}. *IRT1* downregulation was observed in both Col-0 and *almt1* root tips. Iron accumulation in the apoplast occurs in Pi deprived roots as part of the iron-dependent RAM exhaustion mechanism¹³. Thus, *IRT1* downregulation could lead to iron accumulation in the apoplast and, consequently, an enhanced local response to Pi starvation. Further experiments with *irt1* mutants could provide answers about this phenomenon.

CONCLUSIONS

- *low phosphate insensitive 6* is a loss of function mutant line of the *ALUMINUM ACTIVATED MALATE TRANSPORTER 1* gene.
- Seedlings of *almt1* mutant alleles are not able to modify their root architecture in response to Pi deficiency conditions.
- Cell wall related processes, such as lignin deposition and peroxidase activity, are under-regulated in *almt1* root tips in response to Pi deficiency conditions. This processes could contribute to the diminishment of cell wall plasticity, the inhibition of cell growth and the iron accumulation in the root of *Arabidopsis thaliana*.
- *almt1* reversibility revealed a role of malate in the modulation of primary root growth under Pi deficiency conditions.
- *ALMT1* acts upstream of *LPR1* and the iron uptake pathway that triggers the RAM-exhaustion mechanism under Pi deficiency conditions in *Arabidopsis thaliana*.

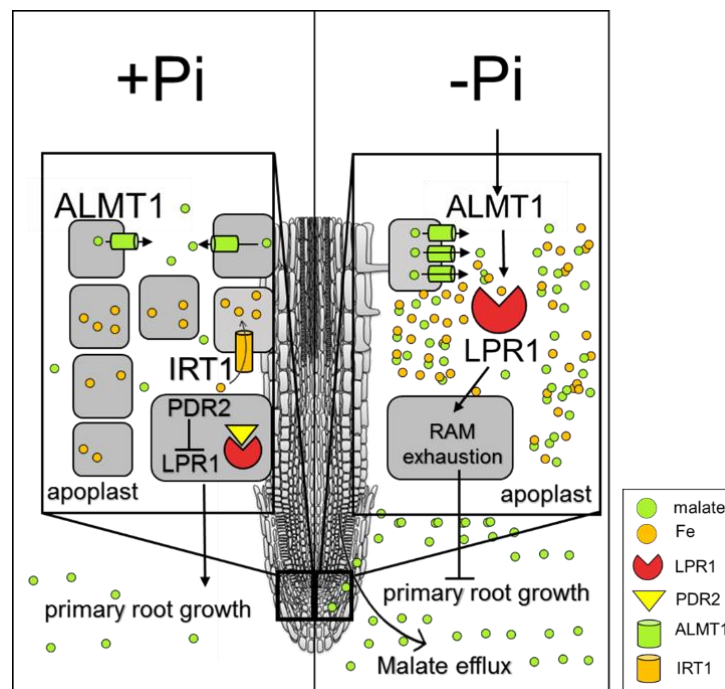


Figure 30. **The *ALMT1* role in the Pi deficiency response.** A proposed role of *ALMT1* in the *LPR1*-dependent RAM exhaustion program in the primary root of *Arabidopsis* is resumed. Malate efflux activated via *ALMT1* induction alters iron distribution in the root which enables *LPR1* activity triggering RAM exhaustion and primary root growth inhibition in *Arabidopsis thaliana* Col-0.

PERSPECTIVES

The generation of transgenic plants harboring a translational construction *ALMT1::GFP* in the Col-0 background would help to the further characterization of the spatio-temporal role of the malate transporter and malate efflux under Pi deficiency conditions.

An isolation of malate-iron complexes using a similar strategy to that of Grillet et al. (2014)⁶⁵, or an *in silico* simulation of the malate-iron complexes that can be formed would provide understanding to the malate-iron interaction mechanism.

Given the role of *ALMT1* in the phosphorus starvation response reported in this work, the overexpression of the malate transporter in *Arabidopsis* transgenic plants seems a natural following step in order to find out if the malate transporter is able to enhance *Arabidopsis* ability to cope with Pi deficiency in the medium, not only in MS plates but in soil conditions. If an overall enhanced tolerance to Pi deficiency conditions is observed it would be interesting to take the study of the over-expression of this gene to commercial crops and contribute to a biotechnological solution for the Pi agricultural challenge.

The application of malate directly to Pi-deficient soil also seems an interesting experiment to test if this organic acid could help plants to assimilate phosphate.

MATERIALS AND METHODS

Plant material

Arabidopsis thaliana Col-0 accession (wild-type) plants were used for the development of this work. *lpi6* EMS-induced homozygous mutants (M2) plants were the object of the characterization for this work. The mutant line was obtained from Mora, J. who isolated and perpetuated the line. Transgenic Col-0 plants with the *proCycB1::GUS³⁸* and *proQC46::GUS³⁸* genetic constructions were used. For the analysis of the marker in the *lpi6* background F3 homozygous mutants resulting from the crosses *lpi6* x Col-0 *proCycB1::GUS³⁸* and *proQC46::GUS³⁸* were used.

A genetic construction harboring the *proALMT1::GFP::GUS* in the Col-0 background was produced. *Arabidopsis* transgenic plants were used using the Gateway cloning system⁶⁷, following primers were used: Fwd-5'-*ggCAGATAAAgAggCACTCgTg-3'* and Rev-5'-*ggTgTTATggAgAAAgtgAgAgAg-3'*. The respective purified PCR products were cloned in pDONR221 and transferred into a pKgWFS7⁶⁸ vector with a GUS::GFP cassette on the same T-DNA, the resultant vector was used for *Agrobacterium*-mediated transformation of *Arabidopsis* ecotype Col-0 plants as previously reported⁶⁹. Transgenic plants (T1) carrying the construction were selected in kanamycin containing (40 µg/mL) media. T2 plants carrying the construction were used for the confocal microscopy analysis of *ALMT1* induction.

Insertional T-DNA *almt1* At1g08430 (SALK_009629; Col-0 background; *almt1*) line was ordered from the Salk Institute (<http://signal.salk.edu/>). At1g02850 T-DNA mutant was ordered from the European Arabidopsis Stock center (NASC N25931; Ler background; *glh11*) (<http://arabidopsis.info/>).

Growing conditions

Seeds were surface sterilized using 95% (v/v) ethanol for 10 min and 20% (v/v) bleach (Cloralex) for 7 min. After three washes in distilled water, seeds were sowed and grown on vertical agar plates for a determinate number of days after germination (dag) in . 0.1× MS medium⁷⁰ containing a low phosphate (-Pi, 5 µM NaH₂PO₄) or high phosphate (+Pi, 100 µM NaH₂PO₄) concentration. For low iron medium, FeSO₄ and Na₂EDTA were replaced

in the nutrient solution by as described by Sanchez-Calderón et al. 2006²³ and Ferrozine (SIGMA) was added up to 100µM final concentration before sterilization. For organic acid supplementation experiments L-malic acid (SIGMA) or L-citric acid (SIGMA) was added up to an interval of 0-1mM final concentration in the medium (for curve experiments) and up to 1 mM malate (+P+M or -P+M) for the characterization of root architectural traits before sterilizing the medium. Agar Plates were vertically placed in a plant growth cabinet (Percival Scientific).

Histochemical staining

3'3-Diaminobenzidine Iron Staining. Iron staining was performed following the methodology reported by Müller et al. 2015^{13,57}. Seedlings were incubated for 30 minutes in 4% (v/v) HCl and 4% Ferrocyanide (Perls staining). 16-well-plates were used for incubation (Corning). DAB intensification was performed by washing the roots after the Perls staining and incubating them for 1 hr in a methanol solution with 10 Mm Na-azide concentration and 0.3% H₂O₂. Seedlings were then washed with 10 mM Na-phosphate buffer at pH 7.4. Wash was followed by a 30-minute incubation in the same buffer containing 0.0025% DAB (SIGMA) and 0.005% H₂O₂. Reaction was stopped by washing with distillate water until no visible trace of DAB in the solution remained. Roots were mounted on glass slides using chloral hydrate at 1 g/mL and 15% glycerol for clarification. Stained roots were photographed using Nomarski optics on a Leica DMR microscope.

B-Glucuronidase activity (GUS) staining. GUS-staining of RAM exhaustion marker lines of cell cycle activity (*proCycB1::GUS*³⁸) and quiescent center identity (*proQC46::GUS*³⁸) was performed as reported by Sánchez-Calderón et al. 2005²³. *Arabidopsis* seedlings were incubated overnight at 37°C in GUS reaction buffer (0.5 mg/mL of 5-bromo-4-chloro-3-indolyl-β-D-glucuronide in 100 mM sodium phosphate solution at pH 7). Stained seedlings were photographed using an Olympus BX43 microscope.

Phloroglucinol staining. Roots were stained for 10 min in 20% HCl ethanol solution at 1% v/v phloroglucinol concentration and observed using Nomarski optics on a Leica DMR microscope.

Mapping by sequencing

Mapping by sequencing was performed using an approach similar to that of Abe et al. 2012³⁹. Pooled whole DNA libraries (MySeq Illumina 2x150pb) from Col-0 and mutant phenotypes were provided by (Mora, J. *unpublished*). Quality assessment of the sequences was performed using FastQC (version 0.11.4; <http://www.bioinformatics.babraham.ac.uk/projects/fastqc/>) and processed using Trimmomatic (version 0.33) to remove reads that contained adapter sequences and low quality reads. Pooled-reads from the DNA-libraries were mapped to the Col-0 reference genome (TAIR10) using Samtools^{71,72} (version 0.1.19) and BWA⁷³ (version 0.7.12). Homozygous variants in the pooled mutant genome were identified using GATK⁷⁴ bioinformatic tool (version 3.1). Candidate genes were determined using VCFtools⁷⁵ (version 0.1.12) and SNPeff⁷⁶ (version 3.6).

The mutated region of the selected candidate (*ALMT1* for *lpi6*) was amplified, PCR products were purified and sequenced using Sanger Sequencing technology. A region of 800 bp flanking the site of the mutation was amplified using the following primers: Fwd: 5'-CAGCTgCgTTgTCGACgTTCgTA-3' and Rev: 5'-AgTCCCCCTTCTCTCTCgCTTCAA-3'.

Root tip definition

Root tip sections of approximately 1 mm length, from the start of the root tip to the beginning of the differentiation zone were collected 5 dag from Col-0 and *almt1(lpi6)* plants.

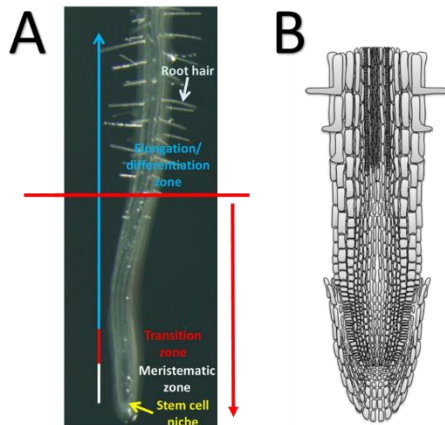


Figure 31. **Root tip.** Sections of root from the start of the root cap to the beginning of the differentiation zone were considered as root tips during the development of this project. (A) Obtained section from the root is highlighted with a red arrow. Picture modified from Takatsuka et al. 2015⁷⁷ (B) Schematic representation of the root section that was considered as root tip during the development of this work.

Preparation of root tip mRNA-seq libraries

Arabidopsis plants were grown on MS agar plates under Pi sufficiency conditions (+P, 100 μ M Pi) and Pi deficiency conditions (-P, 5 μ M Pi). Root tip sections of approximately 1 mm length, from the start of the root tip to the beginning of the differentiation zone were collected 5 dag from Col-0 and *almt1(lpi6)* plants grown under +P and -P conditions. Total RNA was isolated from frozen root tips powder using TRIzol reagent (Invitrogen) and further purified using the Plant RNeasy kit (Qiagen) according to the manufacturer's instructions. Non-strand-specific mRNA-seq libraries were generated from 5 μ g of total RNA and prepared using the TruSeq RNA Sample Prep kit (Illumina) according to the manufacturer's instructions. Sequencing was performed using the NextSeq platform (Illumina), 1 X 75 bp reads were generated.

Mapping and processing of mRNA-seq reads

RNA-Seq bioinformatic analysis was carried out as in Yong-Villalobos (2015)⁷⁸. Quality assessment of the reads generated with the Illumina analysis pipeline (fastQ format) was performed using FastQC (version 0.11.4) and processed using Trimmomatic⁷⁹ (version 0.35) to remove reads that contained adapter sequences and low quality reads. The paired-end clean reads were aligned to the *Arabidopsis thaliana* TAIR10 reference sequence using Bowtie2⁸⁰ (version 2.2.6). The raw counts per gene were estimated by HTseq⁸¹ (version 0.6.1). Data was normalized in edgeR⁸² (version 3.12.0) using the trimmed mean of M values (TMM) method. Genes with ≥ 1 reads in total, across all samples, were included in the final analysis. Transcript abundance as represented by the normalized raw counts per gene was used to determine differential expression using the edgeR⁸² package. Differential expression data is presented in units of logarithm base 2, or logFC, of the relative change of transcript abundance between pairwise comparisons (Col-0 -Pi/+Pi; *almt1* -Pi/+Pi). Differentially expressed genes between samples were filtered using a .05% FDR cutoff and logFC < -2 (downregulated transcripts) or logFC > 2 (for upregulated transcripts) threshold. Gene Ontology analysis graphs were created using REVIGO⁸³ and local and systemic transcriptomic response diagram (Figure 24) was created using GOplot⁸⁴.

The transcriptomic data processing pipeline is presented in Figure 32:

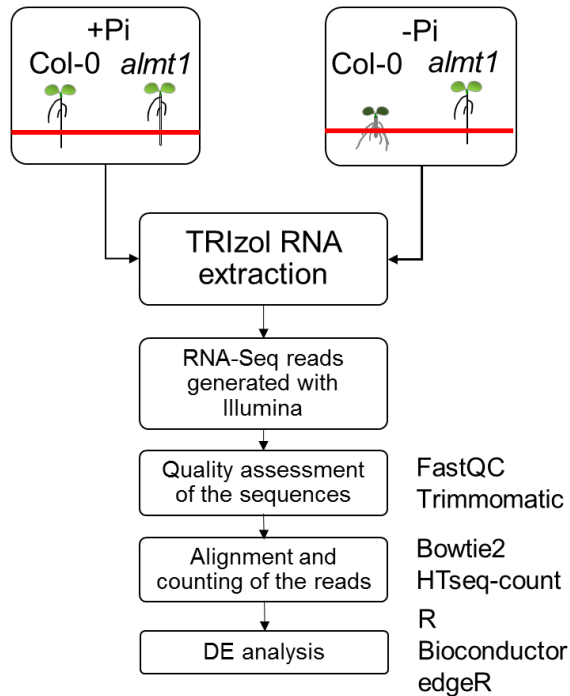


Figure 32. **RNA-seq strategy used for Col-0 and *almt1* transcriptomic profiling under Pi-deficiency conditions.** Preparation of root-tip mRNA-seq libraries and mapping and processing of the reads flow of data is resumed.

qRT-PCR

Total RNA was isolated using TRIzol reagent (Invitrogen) and further purified using the Qiagen RNeasy plant mini kit according to the manufacturer's instructions. Real-time PCR was performed with an Applied Biosystems 7500 real-time PCR system using SYBR Green detection chemistry (Applied Biosystems) and gene-specific primers. The genes ACTIN2 (AtACT2, At3g18780) and UBIQUITIN 10 (UBQ10, At4g05320) served as internal controls. The relative expression levels were computed by the Ct method of relative quantification. Oligonucleotide primer sequences are listed in Table 3.

GENE	PRIMER	SEQUENCE		
PLP2A	Fwd	5'-	CCAACATATATTCGCATCCAGGATGACA	-3'
	Rev	5'-	TGAGGTGAACGAATGTCTCGGATC	-3'
SPX1	Fwd	5'-	CATATGAAGAGCACAATCGCTGCCTTG	-3'
	Rev	5'-	GGCTTCTTGCTCCAACAATGGAATCTTC	-3'
SQD1	Fwd	5'-	CATTGACTCCTATTGCCTCCATT	-3'
	Rev	5'-	TCCCTGTCAAAGCCTTCCAT	-3'
MGDG3	Fwd	5'-	ATGGGAGCAGAGAGGATCAA	-3'
	Rev	5'-	CGAATTCGATCTTAAAAGC	-3'
PDR2	Fwd	5'-	GGAGCACTGAAGCAGGCCCATGTT	-3'
	Rev	5'-	TTGAACATCTGAAGAGTCGTCACAAGT	-3'
ALMT1	Fwd	5'-	GGCCGACCGTGCTATACGAG	-3'
	Rev	5'-	GAGTTGAATTACTACTGAAG	-3'
LPR1	Fwd	5'-	TCAGGGACTACAGAGGTATGGGA	-3'
	Rev	5'-	ACCTTAAGCGGCCTCATCAT	-3'
UBQ10	Fwd	5'-	CGTGCTACAATACTCTAAGCTTCCAAC	-3'
	Rev	5'-	AGAGGTCTCTACGAGAGTTCAAATCCT	-3'
IRT1	Fwd	5'-	CCCGCAAATGATGTTACCTT	-3'
	Rev	5'-	ACTCGGTATCGCAAGAGCTG	-3'

Table 3. Oligonucleotide primer sequences used for qRT-PCR analysis.

Transcriptome validation

Levels of expression of selected genes were determined using qRT-PCR and were compared with the levels of expression reported by RNA-seq transcriptomic data. Similar expression levels were observed between methodologies, which validated our RNA-seq analysis results.

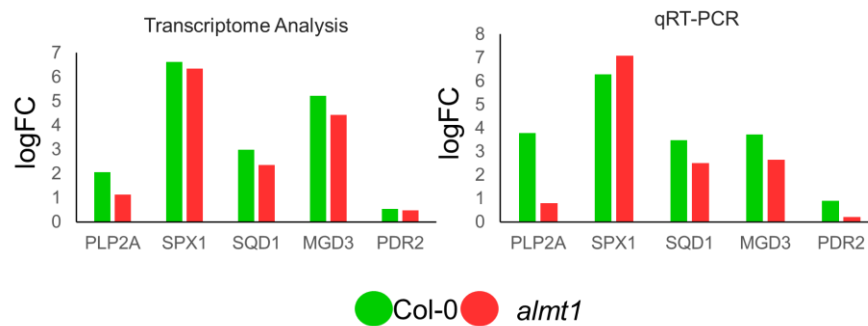


Figure 33. **Transcriptome qRT-PCR validation.** Pairwise comparisons between transcript abundance (*Col-/+*; *almt1 -/+*) were performed, in both transcriptome analysis and qRT-PCR analysis. Overall, the levels of expression were similar including *PDR2* which is a gene that was filtered out by our selection criteria.

GLOSSARY

Abbreviations	
<i>low phosphate insensitive 6</i> mutant	<i>lpi6</i>
3'3-Diaminobenzidine	DAB
base pairs	bp
<i>beta glucosidase 11</i>	<i>glh11</i>
centimeter	cm
Columbia-0 (ecotype; wild type plants)	Col-0
days after germination	dag
ethyl methanesulfonate	EMS
g	grams
Hydrochloric acid	HCl
Inorganic Phosphate	Pi
Iron	Fe
Landsberg erecta (ecotype)	Ler
high phosphate conditions (100 μ M NaH ₂ PO ₄)	+Pi
low phosphate conditions (5 μ M NaH ₂ PO ₄)	-Pi
micrograms	mg
micro-meter	μ m
mililiter	mL
milimeter	mm
milimolar	mM
Murashige and Skoog medium	MS
Phosphorus	P
Root Apical Meristem	RAM
Transference DNA	T-DNA
v	volume
β -glucoronidase	GUS
base two logarithm log ₂ of fold change	LogFC
Fold Change	FC
The Arabidopsis Information Resource	TAIR
TAIR Reference Genome Data Version 10	TAIR10
Locus Identifier (TAIR)	atID
Locus Identifier (TAIR)	ID
False Discovery Rate	FDR
<i>aluminum activated malate transporter 1</i> mutant	<i>almt1</i>

BIBLIOGRAPHY

1. Rubio, V. *et al.* A conserved MYB transcription factor involved in phosphate starvation signaling both in vascular plants and in unicellular algae. *Genes Dev.* **15**, 2122–2133 (2001).
2. Thibaud, M. C. *et al.* Dissection of local and systemic transcriptional responses to phosphate starvation in Arabidopsis. *Plant J.* **64**, 775–789 (2010).
3. Bustos, R. *et al.* A Central Regulatory System Largely Controls Transcriptional Activation and Repression Responses to Phosphate Starvation in Arabidopsis. *PLoS Genet.* **6**, e1001102 (2010).
4. Jain, A., Nagarajan, V. K. & Raghothama, K. G. Transcriptional regulation of phosphate acquisition by higher plants. *Cell. Mol. Life Sci.* **69**, 3207–3224 (2012).
5. Sánchez-Calderón, L. *et al.* Phosphate starvation induces a determinate developmental program in the roots of Arabidopsis thaliana. *Plant Cell Physiol.* **46**, 174–84 (2005).
6. Lopez-Bucio, J. *et al.* Phosphate Availability Alters Architecture and Causes Changes in Hormone Sensitivity in the Arabidopsis Root System. *Plant Physiol.* **129**, 244–256 (2002).
7. Péret, B. *et al.* Root developmental adaptation to phosphate starvation: better safe than sorry. *Trends Plant Sci.* **16**, 442–450 (2011).
8. Bates, T. R. & Lynch, J. P. Stimulation of root hair elongation in Arabidopsis thaliana by low phosphorus availability. *Plant, Cell Environ.* **19**, 529–538 (1996).
9. Lynch, J. P. Root Phenotypes for Enhanced Soil Exploration and Phosphorus Acquisition: Tools for Future Crops. *Plant Physiol.* **156**, 1041–1049 (2011).
10. Jianbo, S. *et al.* Phosphorus Dynamics: From Soil to Plant. *Plant Physiol.* **156**, 997–1005 (2011).
11. Hoekenga, O. A. *et al.* AtALMT1, which encodes a malate transporter, is identified as one of several genes critical for aluminum tolerance in Arabidopsis. *Proc. Natl. Acad. Sci.* **103**, 9738–9743 (2006).
12. Kobayashi, Y. *et al.* Characterization of AtALMT1 expression in aluminum-inducible malate release and its role for rhizotoxic stress tolerance in Arabidopsis. *Plant Physiol.* **145**, 843–852 (2007).
13. Müller, J. *et al.* Iron-Dependent Callose Deposition Adjusts Root Meristem Maintenance to Phosphate Availability. *Dev. Cell* **33**, 216–230 (2015).
14. Cakmak, I. in *Progress in Plant Nutrition: Plenary Lectures of the XIV International Plant Nutrition Colloquium 3–24* (Springer Netherlands, 2002). doi:10.1007/978-94-017-2789-1_1
15. Elser, J. & Bennett, E. Phosphorus cycle: A broken biogeochemical cycle. *Nature* **478**, 29–31 (2011).
16. Cordell, D., Drangert, J. O. & White, S. The story of phosphorus: Global food security and food for thought. *Glob. Environ. Chang.* **19**, 292–305 (2009).
17. Gilbert, N. Environment: The disappearing nutrient. *Nature* **461**, 716–718 (2009).

18. Koppelaar, R. H. E. M. & Weikard, H. P. Assessing phosphate rock depletion and phosphorus recycling options. *Glob. Environ. Chang.* **23**, 1454–1466 (2013).
19. Raghothama, K. G. Phosphate Acquisition. *Annu Rev Plant Physiol Plant Mol Biol* **50**, 665–693 (1999).
20. Barber, S. A., Walker, J. M. & Vasey, E. H. Mechanisms for Movement of Plant Nutrients from Soil and Fertilizer to Plant Root. *J. Agric. Food Chem.* **11**, 204–207 (1963).
21. Hinsinger, P. Bioavailability of soil inorganic P in the rhizosphere as affected by root-induced chemical changes: a review. *Plant Soil* **237**, 173–195 (2001).
22. Herrera-Estrella, L. *et al.* Phosphorus: The Underrated Element for Feeding the World. *Trends Plant Sci.* **21**, 461–463 (2016).
23. Sanchez-Calderon, L. Phosphate Starvation Induces a Determinate Developmental Program in the Roots of *Arabidopsis thaliana*. *Plant Cell Physiol.* **46**, 174–184 (2005).
24. Lin, W.-Y., Lin, S.-I. & Chiou, T.-J. Molecular regulators of phosphate homeostasis in plants. *J. Exp. Bot.* **60**, 1427–38 (2009).
25. Miura, K. *et al.* The *Arabidopsis* SUMO E3 ligase SIZ1 controls phosphate deficiency responses. *Proc. Natl. Acad. Sci. U. S. A.* **102**, 7760–5 (2005).
26. Bari, R., Pant, B. D., Stitt, M. & Scheible, W.-R. PHO2, MicroRNA399, and PHR1 Define a Phosphate-Signaling Pathway in Plants. *Plant Physiol.* **141**, 988–999 (2006).
27. Barabote, R. D. *et al.* Extra domains in secondary transport carriers and channel proteins. *Biochim. Biophys. Acta - Biomembr.* **1758**, 1557–1579 (2006).
28. Secco, D. *et al.* The emerging importance of the SPX domain-containing proteins in phosphate homeostasis. *New Phytol.* **193**, 842–851 (2012).
29. Puga, M. I. *et al.* SPX1 is a phosphate-dependent inhibitor of PHOSPHATE STARVATION RESPONSE 1 in *Arabidopsis*. *Proc. Natl. Acad. Sci.* **111**, 14947–14952 (2014).
30. Nussaume, L. *et al.* Phosphate Import in Plants: Focus on the PHT1 Transporters. *Front. Plant Sci.* **2**, 83 (2011).
31. Plaxton, W. C. & Tran, H. T. Metabolic Adaptations of Phosphate-Starved Plants. *Plant Physiol.* **156**, 1006–1015 (2011).
32. Cruz-Ramirez, A., Oropeza-Aburto, A., Razo-Hernandez, F., Ramirez-Chavez, E. & Herrera-Estrella, L. Phospholipase DZ2 plays an important role in extraplastidic galactolipid biosynthesis and phosphate recycling in *Arabidopsis* roots. *Proc. Natl. Acad. Sci.* **103**, 6765–6770 (2006).
33. Oropeza-Aburto, A. *et al.* Functional analysis of the *Arabidopsis* PLDZ2 promoter reveals an evolutionarily conserved low-Pi-responsive transcriptional enhancer element. *J. Exp. Bot.* **63**, 2189–202 (2012).
34. Pant, B. D. *et al.* The transcription factor PHR1 regulates lipid remodeling and triacylglycerol accumulation in *Arabidopsis thaliana* during phosphorus starvation. *J. Exp. Bot.* **66**, 1907–18 (2015).
35. Svistoonoff, S. *et al.* Root tip contact with low-phosphate media reprograms plant root architecture. *Nat. Genet.* **39**, 792–796 (2007).

36. Ticconi, C. A. *et al.* ER-resident proteins PDR2 and LPR1 mediate the developmental response of root meristems to phosphate availability. *Proc. Natl. Acad. Sci.* **106**, 14174–14179 (2009).
37. Ward, J. T., Lahner, B., Yakubova, E., Salt, D. E. & Raghothama, K. G. The effect of iron on the primary root elongation of Arabidopsis during phosphate deficiency. *Plant Physiol.* **147**, 1181–91 (2008).
38. Sabatini, S. *et al.* An Auxin-Dependent Distal Organizer of Pattern and Polarity in the Arabidopsis Root. *Cell* **99**, 463–472 (1999).
39. Abe, A. *et al.* Genome sequencing reveals agronomically important loci in rice using MutMap. *Nat. Biotechnol.* **30**, 174–178 (2012).
40. Kochian, L. V., Hoekenga, O. A. & Piñeros, M. A. How do crop plants tolerate acid soils? Mechanisms of aluminum tolerance and phosphorus efficiency. *Annu. Rev. Plant Biol* **55**, 459–93 (2004).
41. Liang, C. *et al.* Low pH, Aluminum, and Phosphorus Coordinately Regulate Malate Exudation through GmALMT1 to Improve Soybean Adaptation to Acid Soils. *Plant Physiol.* **161**, 1347–1361 (2013).
42. Xu, Z. *et al.* Functional genomic analysis of Arabidopsis thaliana glycoside hydrolase family 1. *Plant Mol. Biol.* **55**, 343–367 (2004).
43. Miura, K. *et al.* SIZ1 Regulation of Phosphate Starvation-Induced Root Architecture Remodeling Involves the Control of Auxin Accumulation. *Plant Physiol.* **155**, 1000–1012 (2011).
44. Sitia, R. & Braakman, I. Quality control in the endoplasmic reticulum protein factory. *Nature* **426**, 891–894 (2003).
45. Raes, J., Rohde, A., Christensen, J. H., Van de Peer, Y. & Boerjan, W. Genome-wide characterization of the lignification toolbox in Arabidopsis. *Plant Physiol.* **133**, 1051–71 (2003).
46. Cosgrove, D. J. Growth of the plant cell wall. *Nat. Rev. Mol. Cell Biol.* **6**, 850–861 (2005).
47. Francoz, E. *et al.* Roles of cell wall peroxidases in plant development. *Phytochemistry* **112**, 15–21 (2015).
48. Hoehenwarter, W. *et al.* Comparative expression profiling reveals a role of the root apoplast in local phosphate response. *BMC Plant Biol.* **16**, 106 (2016).
49. Ziegler, J. *et al.* Non-targeted profiling of semi-polar metabolites in Arabidopsis root exudates uncovers a role for coumarin secretion and lignification during the local response to phosphate limitation. *J. Exp. Bot.* **67**, 1421–32 (2016).
50. Wu, P. *et al.* Phosphate Starvation Triggers Distinct Alterations of Genome Expression in Arabidopsis Roots and Leaves. *PLANT Physiol.* **132**, 1260–1271 (2003).
51. AL-GHAZI, Y. *et al.* Temporal responses of Arabidopsis root architecture to phosphate starvation: evidence for the involvement of auxin signalling. *Plant, Cell Environ.* **26**, 1053–1066 (2003).
52. Hoffland, e., Boogaard, r., Nelemans, j. & Findenegg, G. Biosynthesis and root exudation of citric and malic acids in phosphate-starved rape plants. *New Phytol.* **122**, 675–680 (2006).

53. Neumann, G. & Römheld, V. Root excretion of carboxylic acids and protons in phosphorus-deficient plants. *Plant Soil* **211**, 121–130 (1999).
54. Langlade, N. B. *et al.* ATP citrate lyase: cloning, heterologous expression and possible implication in root organic acid metabolism and excretion. *Plant, Cell Environ.* **25**, 1561–1569 (2002).
55. Durrett, T. P., Gassmann, W. & Rogers, E. E. The FRD3-Mediated Efflux of Citrate into the Root Vasculature Is Necessary for Efficient Iron Translocation. *Plant Physiol.* **144**, 197–205 (2007).
56. Rellán-Alvarez, R. *et al.* Identification of a tri-iron(III), tri-citrate complex in the xylem sap of iron-deficient tomato resupplied with iron: new insights into plant iron long-distance transport. *Plant Cell Physiol.* **51**, 91–102 (2010).
57. Roschztardt, H., Conejero, G., Curie, C. & Mari, S. Identification of the Endodermal Vacuole as the Iron Storage Compartment in the Arabidopsis Embryo. *Plant Physiol.* **151**, 1329–1338 (2009).
58. Meyer, S. *et al.* Intra- and extra-cellular excretion of carboxylates. *Trends Plant Sci.* **15**, 40–7 (2010).
59. Kanno, S. *et al.* A novel role for the root cap in phosphate uptake and homeostasis. *Elife* **5**, (2016).
60. Velasquez, S. M. *et al.* O-glycosylated cell wall proteins are essential in root hair growth. *Science* **332**, 1401–3 (2011).
61. Cosgrove, D. J. Loosening of plant cell walls by expansins. *Nature* **407**, 321–6 (2000).
62. Passardi, F., Penel, C. & Dunand, C. Performing the paradoxical: how plant peroxidases modify the cell wall. *Trends Plant Sci.* **9**, 534–540 (2004).
63. Jones, D. Organic acids in the rhizosphere - a critical review. *Plant Soil* **205**, 25–44 (1998).
64. Taylor-Teeples, M. *et al.* An Arabidopsis gene regulatory network for secondary cell wall synthesis. *Nature* **517**, 571–5 (2015).
65. Grillet, L. *et al.* Ascorbate efflux as a new strategy for iron reduction and transport in plants. *J. Biol. Chem.* **289**, 2515–25 (2014).
66. Li, W. *et al.* Genome-wide analysis of overlapping genes regulated by iron deficiency and phosphate starvation reveals new interactions in Arabidopsis roots. *BMC Res. Notes* **8**, 555 (2015).
67. Hartley, J. L., Temple, G. F. & Brasch, M. A. DNA cloning using in vitro site-specific recombination. *Genome Res.* **10**, 1788–95 (2000).
68. Karimi, M., Inzé, D. & Depicker, A. GATEWAY™ vectors for Agrobacterium-mediated plant transformation. *Trends Plant Sci.* **7**, 193–195 (2002).
69. Martínez-Trujillo, M., Limones-Briones, V., Cabrera-Ponce, J. L. & Herrera-Estrella, L. Improving transformation efficiency of Arabidopsis thaliana by modifying the floral dip method. *Plant Mol. Biol. Report.* **22**, 63–70 (2004).
70. Murashige, T. & Skoog, F. A Revised Medium for Rapid Growth and Bio Assays with Tobacco Tissue Cultures. *Physiol. Plant.* **15**, 473–497 (1962).

71. Li, H. *et al.* The Sequence Alignment/Map format and SAMtools. *Bioinformatics* **25**, 2078–9 (2009).
72. Li, H. A statistical framework for SNP calling, mutation discovery, association mapping and population genetical parameter estimation from sequencing data. *Bioinformatics* **27**, 2987–93 (2011).
73. Li, H. & Durbin, R. Fast and accurate long-read alignment with Burrows-Wheeler transform. *Bioinformatics* **26**, 589–95 (2010).
74. McKenna, A. *et al.* The Genome Analysis Toolkit: A MapReduce framework for analyzing next-generation DNA sequencing data. *Genome Res.* **20**, 1297–1303 (2010).
75. Danecek, P. *et al.* The variant call format and VCFtools. *Bioinformatics* **27**, 2156–8 (2011).
76. Cingolani, P. *et al.* A program for annotating and predicting the effects of single nucleotide polymorphisms, SnpEff. <http://dx.doi.org/10.4161/fly.19695> (2012).
77. Takatsuka, H. & Umeda, M. Epigenetic Control of Cell Division and Cell Differentiation in the Root Apex. *Front. Plant Sci.* **6**, 1178 (2015).
78. Yong-Villalobos, L. *et al.* Methylome analysis reveals an important role for epigenetic changes in the regulation of the *Arabidopsis* response to phosphate starvation. *Proc. Natl. Acad. Sci.* **112**, E7293–E7302 (2015).
79. Bolger, A. M., Lohse, M. & Usadel, B. Trimmomatic: a flexible trimmer for Illumina sequence data. *Bioinformatics* **30**, 2114–20 (2014).
80. Langmead, B. *et al.* Ultrafast and memory-efficient alignment of short DNA sequences to the human genome. *Genome Biol.* **10**, R25 (2009).
81. Anders, S., Pyl, P. T. & Huber, W. HTSeq—a Python framework to work with high-throughput sequencing data. *Bioinformatics* **31**, 166–9 (2015).
82. Robinson, M. D., McCarthy, D. J. & Smyth, G. K. edgeR: a Bioconductor package for differential expression analysis of digital gene expression data. *Bioinformatics* **26**, 139–40 (2010).
83. Supek, F., Bošnjak, M., Škunca, N. & Šmuc, T. REVIGO Summarizes and Visualizes Long Lists of Gene Ontology Terms. *PLoS One* **6**, e21800 (2011).
84. Walter, W., Sánchez-Cabo, F. & Ricote, M. GOplot: an R package for visually combining expression data with functional analysis. *Bioinformatics* **31**, 2912–4 (2015).
85. Hart, M. R., Quin, B. F. & Nguyen, M. L. Phosphorus runoff from agricultural land and direct fertilizer effects: a review. *J. Environ. Qual.* **33**, 1954–72
86. Yan, Z., Chen, S., Li, J., Alva, A. & Chen, Q. Manure and nitrogen application enhances soil phosphorus mobility in calcareous soil in greenhouses. *J. Environ. Manage.* **181**, 26–35 (2016).
87. Hamburger, D., Rezzonico, E., MacDonald-Comber Petétot, J., Somerville, C. & Poirier, Y. Identification and characterization of the *Arabidopsis* PHO1 gene involved in phosphate loading to the xylem. *Plant Cell* **14**, 889–902 (2002).
88. Stefanovic, A. *et al.* Over-expression of PHO1 in *Arabidopsis* leaves reveals its role in mediating phosphate efflux. *Plant J.* **66**, 689–699 (2011).

89. Wang, Y., Ribot, C., Rezzonico, E. & Poirier, Y. Structure and expression profile of the Arabidopsis PHO1 gene family indicates a broad role in inorganic phosphate homeostasis. *Plant Physiol.* **135**, 400–11 (2004).
90. Ramesh, S. A. *et al.* GABA signalling modulates plant growth by directly regulating the activity of plant-specific anion transporters. *Nat. Commun.* **6**, 7879 (2015).
91. Barros, J., Serk, H., Granlund, I. & Pesquet, E. The cell biology of lignification in higher plants. *Ann. Bot.* **115**, 1053–74 (2015).
92. Sauter, M. & Kende, H. Levels of β -Glucan and Lignin in Elongating Internodes of Deepwater Rice. *Plant Cell Physiol.* **33**, 1089–1097 (1992).
93. Lequeux, H., Hermans, C., Lutts, S. & Verbruggen, N. Response to copper excess in Arabidopsis thaliana: Impact on the root system architecture, hormone distribution, lignin accumulation and mineral profile. *Plant Physiol. Biochem.* **48**, 673–682 (2010).
94. Hart, M. R., Quin, B. F. & Nguyen, M. L. Phosphorus runoff from agricultural land and direct fertilizer effects: a review. *J. Environ. Qual.* **33**, 1954–72
95. Chaoui, A., Jarrar, B. & EL Ferjani, E. Effects of cadmium and copper on peroxidase, NADH oxidase and IAA oxidase activities in cell wall, soluble and microsomal membrane fractions of pea roots. *J. Plant Physiol.* **161**, 1225–1234 (2004).
96. van de Mortel, J. E. *et al.* Expression differences for genes involved in lignin, glutathione and sulphate metabolism in response to cadmium in Arabidopsis thaliana and the related Zn/Cd-hyperaccumulator Thlaspi caerulescens. *Plant. Cell Environ.* **31**, 301–24 (2008).